24) Yan H, Bigner DD, Velculescu V, Parsons DW: Mutant metabolic enzymes are at the origin of gliomas. *Cancer Res* 69: 9157–919, 2009
25) Yan H, Parsons DW, Jin G, McLendon R, Rasheed BA, Yuan W, Kos I, Batinic-Haberle I, Jones S, Riggins GJ, Friedman H, Friedman A, Reardon D, Herndon J, Kinzler KW, Velculescu VE, Vogelstein B, Bigner DD: IDH1 and IDH2 mutations in gliomas. *N Engl J Med* 360: 765–773, 2009
26) Ward PS, Cross JR, Lu C, Weigert O, Abel-Wahab O, Levine RL, Weinstock DM, Sharp KA, Thompson CB: Identification of additional IDH mutations associated with oncometabolite R(-)-2-hydroxyglutarate production. *Oncogene* 31: 2491–2498, 2012
27) Ward PS, Patel J, Wise DR, Abdel-Wahab O, Bennett BD, Coller HA, Cross JR, Fantin VR, Hedvat CV, Perl AE, Rabinowitz JD, Carroll M, Su SM, Sharp KA, Levine RL, Thompson CB: The common feature of leukemia-associated IDH1 and IDH2 mutations is a neomorphic enzyme activity converting alpha-ketoglutarate to 2-hydroxyglutarate. *Cancer Cell* 17: 225–234, 2010
28) Zhu J, Cui G, Chen M, Xu Q, Wang X, Zhou D, Lv S, Fu L, Wang Z, Zuo J: Expression of R132H mutational IDH1 in human U87 glioblastoma cells affects the SREBP1a pathway and induces cellular proliferation. *J Mol Neurosci* 50: 165–171, 2013

Address reprint requests to: Satsuki Miyata, MD, Department of Neurosurgery, Jichi Medical University, 3311-1 Yakushiji, Shimotsuke, Tochigi 329-0498, Japan.
e-mail: smiyata@jichi.ac.jp

PLOS ONE

Prophylaxis and Treatment of Alzheimer's Disease by Delivery of an Adeno-Associated Virus Encoding a Monoclonal Antibody Targeting the Amyloid Beta Protein

Masaru Shimada[1], Shinya Abe[1], Toru Takahashi[1], Kazumasa Shiozaki[2], Mitsue Okuda[3], Hiroaki Mizukami[4], Dennis M. Klinman[5], Keiya Ozawa[4], Kenji Okuda[1]*

1 Department of Molecular Biodefense Research, Yokohama City University, Yokohama, Kanagawa, Japan, **2** Department of Psychiatry, Yokohama City University, Yokohama, Kanagawa, Japan, **3** Okuda Dental Clinic, Yokohama, Kanagawa, Japan, **4** Division of Genetic Therapeutics, Center for Molecular Medicine, Jichi Medical School, Tochigi-ken, Japan, **5** Laboratory of Experimental Immunology, Cancer and Inflammation Program, National Cancer Institute, National Institutes of Health, Frederick, Maryland, United States of America

Abstract

We previously reported on a monoclonal antibody (mAb) that targeted amyloid beta (Aß) protein. Repeated injection of that mAb reduced the accumulation of Aß protein in the brain of human Aß transgenic mice (Tg2576). In the present study, cDNA encoding the heavy and light chains of this mAb were subcloned into an adeno-associated virus type 1 (AAV) vector with a 2A/furin adapter. A single intramuscular injection of 3.0×10^{10} viral genome of these AAV vectors into C57BL/6 mice generated serum anti-Aß Ab levels up to 0.3 mg/ml. Anti-Aß Ab levels in excess of 0.1 mg/ml were maintained for up to 64 weeks. The effect of AAV administration on Aß levels in vivo was examined. A significant decrease in Aß levels in the brain of Tg2576 mice treated at 5 months (prophylactic) or 10 months (therapeutic) of age was observed. These results support the use of AAV vector encoding anti-Aß Ab for the prevention and treatment of Alzheimer's disease.

Citation: Shimada M, Abe S, Takahashi T, Shiozaki K, Okuda M, et al. (2013) Prophylaxis and Treatment of Alzheimer's Disease by Delivery of an Adeno-Associated Virus Encoding a Monoclonal Antibody Targeting the Amyloid Beta Protein. PLoS ONE 8(3): e57606. doi:10.1371/journal.pone.0057606

Editor: Weidong Le, Baylor College of Medicine, Jiao Tong University School of Medicine, United States of America

Received November 10, 2012; **Accepted** January 23, 2013; **Published** March 28, 2013

Funding: This work was supported in part by a grant-in-aid for the Ministry of Education, Science, Sports, Culture of Japan, and the Ministry of Health and Welfare of Japan. The funders had no role in study design, data collection and analysis, decision to publish, or preparation of the manuscript.

Competing Interests: The authors have declared that no competing interests exist.

* E-mail: kokuda@chojuken.net

Introduction

Alzheimer's disease (AD) is a disorder characterized by a diffuse loss of neurons and the accumulation of amyloid beta (Aß) protein, followed by the production of tau protein or senile plaques in the brain [1–2]. Active immunization with Aß peptide was found to reduce the amyloid burden and improve cognitive behavior in murine AD models [3–4].

Clinical trials involving peptide immunization were suspended owing to the development of meningioencephalitis in some volunteers vaccinated with Aß peptide [5–6]. Clinical studies and autopsy results indicated aseptic meningoencephalitis, presumably induced by the T-cell responses [6–8]. Of note, several of the samples obtained from vaccinated patients demonstrated a remarkable reduction in Aß protein levels and senile plaque formation [9–10]. These results suggest that if the adverse side effects of such therapy could be avoided, immune mediated elimination of Aß protein could represent a promising therapy for AD.

Based on these observations, the efficacy of intravenous delivery of humanized monoclonal antibodies (mAbs) against Aß was examined [11–13]. Despite the widespread reduction in Aß plaques, the passive transfer of mAb reduced AD-like symptoms in only a subset of patients [10]. This observation suggests that neuronal degeneration may occur during the early stages of AD, before the appearance of large Aß aggregates. Thus, it is important to eliminate Aß oligomers at the earliest stages of AD. Previously, we developed a mAb targeting the Aß1–13 peptide. Prophylactic delivery of this mAb or its F(ab')2 fragments to human Aß transgenic mice (Tg2576) effectively prevented the accumulation of Aß protein and plaques [14]. However, Pfeifer et al. [15] reported that anti-Aß mAb treatment could also lead to microhemorrhages in APP23 mice. Moreover, repeated high-dose mAb injections are likely to be very expensive [5,8].

A potentially safer and more efficacious strategy would be to inject an adeno-associated virus (AAV) that leads to the continuous production of anti-Aß mAb over an extended period. AAV is a nonpathogenic and poorly immunogenic virus. When used as a vector, it can transfer a gene of interest to non-dividing mammalian cells resulting in persistent transgene expression [16].

This work examines the feasibility of using an AAV vector type 1 (AAV vector) modified to encode the anti-Aß Ab to prevent or treat AD in mice. This approach avoids the need to repeatedly administer high doses of mAb. Results suggest that therapy with an Aß mAb-expressing AAV vector greatly reduce Aß accumulation in AD model mice.

Results

Production of Ab by cells transfected with the Aß mAb – expressing AAV vector

We first determined whether the transduction of the new Aß mAb – expressing AAV vector resulted in the production of mAb by HEK293 cells. As shown in Figure 1, we detected Abs in the cell lysates and culture supernatant of the transduced cells. Heavy (H) and Light (L) chains of the appropriate molecular weight were detected. In addition, we detected intact Ab under non – reducing condition. These results indicate that Aß mAb – expressing AAV vector-transduced cells produce proteins with the molecular weight of Abs.

Binding activity of the Ab produced by AAV vector – transduced cells

We next assessed whether the HEK293 – derived Abs could bind to monomeric Aß protein and oligomerized Aß protein similar to those found in the brain of patients with AD [17]. Results show that culture supernatant derived from Aß mAb-expressing AAV vector-transduced HEK293 cells bound to monomers, dimers, trimers, and tetramers of Aß protein (Figure 2A).

We then analyzed whether Aß mAb – expressing vector-produced Abs bound to Aß aggregates by observing sliced brain sections from Tg2576 mice. Aß aggregates were clearly detected in the brain sections using a polyclonal antibody against Aß1 – 42, anti – Aß1–13 mAb (IIA2), and the culture supernatant from Aß mAb – expressing vector – transduced HEK293 cells (Figure 2B). These results suggest that functional anti-Aß mAb is produced by cells transduced with this Aß mAb – expressing vector.

Inhibition of hippocampal cell death by Aß aggregates using culture supernatant from AAV-transduced cells

It is hypothesized that early AD is characterized by the aggregation of Aß protein, and is followed by abnormal tau phosphorylation leading to massive neuronal cell death in the brain. We therefore examined whether the culture supernatant from Aß mAb - expressing AAV vector-transduced cells could inhibit the death of primary hippocampal cells. As shown in Figure 3, synthetic soluble Aß aggregates killed hippocampal cells. This cell death was significantly reduced by the addition of culture supernatant from Aß mAb - expressing vector-transduced cells at 6 h and 24 h after incubation. These results suggest that the culture supernatant of AAV-transduced cells can inhibit the death of primary hippocampal cells.

Antibody titers of mice infected with the Aß mAb-expressing AAV vector

Ten weeks old C57BL/6 mice were intramuscularly (i.m.) injected with 3.0×10^{9}, 3.0×10^{10} or 3.0×10^{11} viral genome (vg) of the Aß mAb - expressing vector or 3.0×10^{11} vg of LacZ-expressing vector. After administration, serum from these mice was collected monthly and antibody titers were assayed for 64 weeks (Figure 4). Anti-Aß Ab titers peaked approximately 4 weeks after administration and then slowly declined, remaining detectable through 64 weeks of follow up. Ab titers were dose-dependent, with the greatest amount of Ab being present in mice treated with 10^{11} vg of the Aß mAb-expressing AAV vector. In contrast, no Aß-specific Abs were detected in mice injected with the LacZ-expressing AAV vector (data not shown). By 64-week post administration, 0.1 mg/ml of Aβ-specific Ab can be detected in the mice administrated with 3.0×10^{10} vg of the Aß mAb-expressing AAV vector. Considering the safe dosage range of 2.1×10^{12}–6.9×10^{13} vg/individual [18] and 2×10^{11}–1.8×10^{12} vg/kg [19] in phase 1 clinical trials of intramuscular injection of the recombinant AAV vector, we use the dose of 3.0×10^{10} vg/mouse for further in vivo study, based on the body weight ratio of human beings (60 kg) vs mouse (20 g) and the Ab titer after administration of Aβ mAb-expressing AAV vector (Figure 4).

Effect of Aß mAb-expressing AAV vector prophylaxis on Tg2576 mice

To determine whether the Aß mAb-expressing AAV vector was able to prevent Tg2576 mice from developing AD, 5-month old animals were injected once with 3.0×10^{10} vg of this vector. Whereas no Aβ protein accumulated in normal mice, there was a statistically significant increase in the amount of Aβ1-40 and Aβ1-42 present in the brain of Tg2576 animals treated with the control LacZ-expressing vector by 10 months of age. The accumulation of this protein continued to rise over time (Figure 5B). By comparison, the amount of Aβ protein present

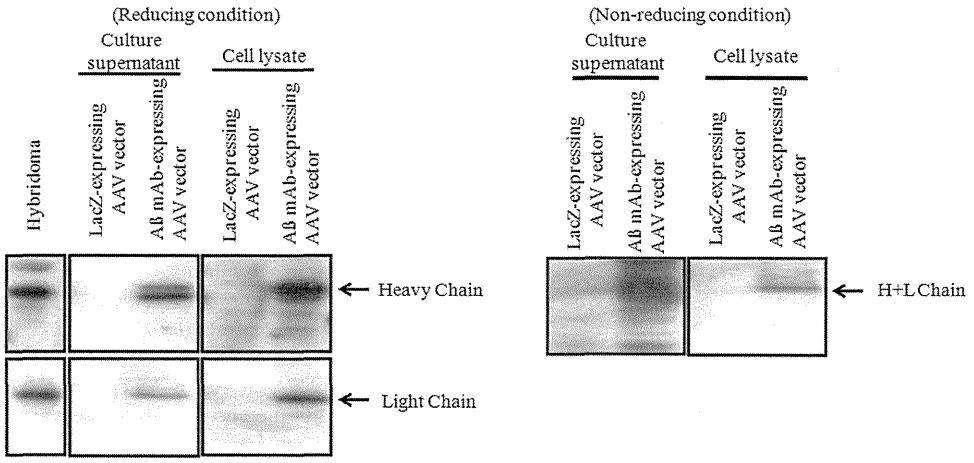

Figure 1. In vitro expression of anti - Aß Abs following the transduction of HEK293 cells with the Aß mAb – expressing AAV vector. Western blots of culture supernatant and cell lysates identify the Ig light and heavy chain (under reducing conditions) and whole Ab (under non-reducing conditions). Cells transfected with a LacZ encoding AAV vector served as negative controls.
doi:10.1371/journal.pone.0057606.g001

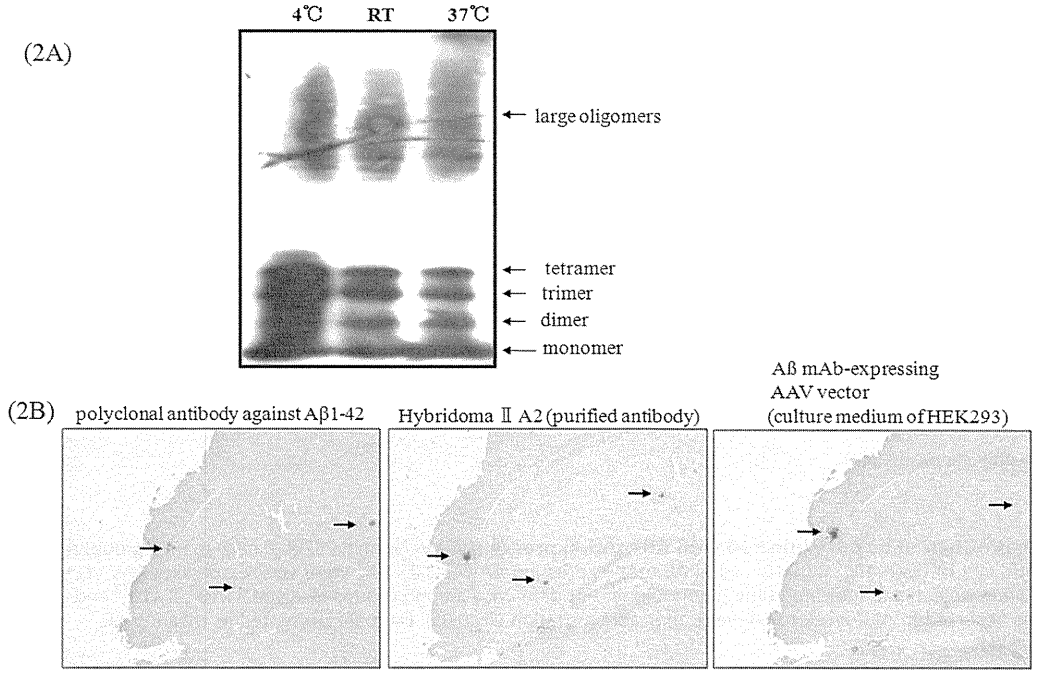

Figure 2. Binding activity of the Ab produced by Aß mAb – expressing AAV vector-transduced cells. A) Binding of Ab from Aß mAb – expressing AAV vector transduced HEK293 cells to synthetic Aß peptides, monomers and oligomers by Western blot. The Ab1-42 peptide was aggregated at 4°C, room temperature (R.T.), or 37°C as described in Materials and Methods and detected by culture supernatant derived from Aß mAb – expressing AAV vector transduced HEK293 cells. B) Anti – Aß Ab derived from transduced HEK293 bound to Aß plaques in 16-month old Tg2576 mice. The specificity of this binding was confirmed by use of polyclonal and monoclonal Abs (see details in Materials and Methods).
doi:10.1371/journal.pone.0057606.g002

in Tg2576 mice treated with the Aβ mAb-expressing AAV vector was significantly and persistently reduced (Figure 5B).

Serial sagital sections were prepared from the brains of these animals. Aß protein deposits were then visualized immunohistochemically in these sections. Both the size and number of Aβ protein containing deposits increased over time in Tg mice treated with the LacZ-expressing vector. The number of such plaques was significantly reduced among mice treated with the Aß mAb-expressing vector (Figure 5C).

Effect of Aß mAb-expressing AAV vector treatment on Tg2576 mice

We finally sought to determine whether the Aß mAb-expressing AAV vector could be used therapeutically. Ten-month old animals were injected with 3.0×10^{10} vg of vector. Aß protein continued to accumulate at 13 months in mice treated with either the LacZ or Aß mAb-expressing AAV vector. However by 15 months (and continuing through 17 months) the size and number of Aß protein containing deposits in the brains of animals treated with the Aß mAb-expressing vector was significantly reduced when compared to LacZ controls (Figure 6B). This divergence was confirmed

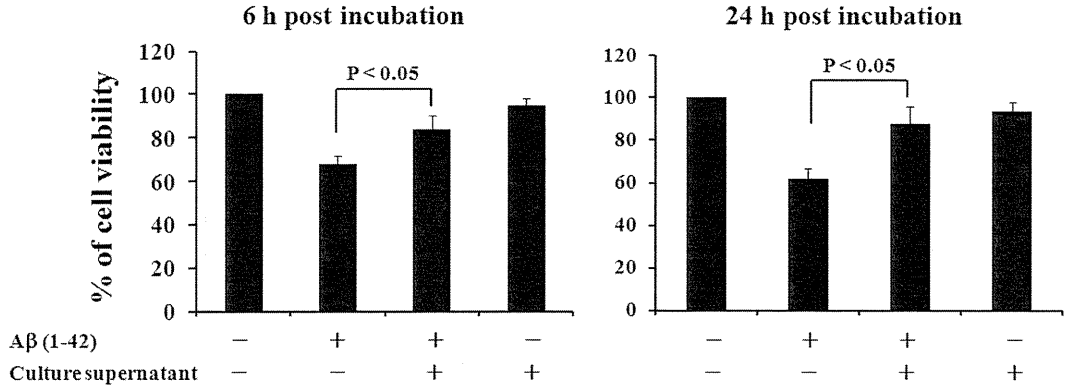

Figure 3. In vitro cytotoxicity inhibition test using primary culture hippocampal cells. The viability of primary hippocampal cells after 6–24 h of culture with 10 uM aggregated Aß protein was examined. The effect of adding culture supernatant from Aß mAb - expressing AAV vector transduced cells was also examined by MTT assay. Data represent the results of 5–8 independently analyzed samples and are presented as mean ± SE.
doi:10.1371/journal.pone.0057606.g003

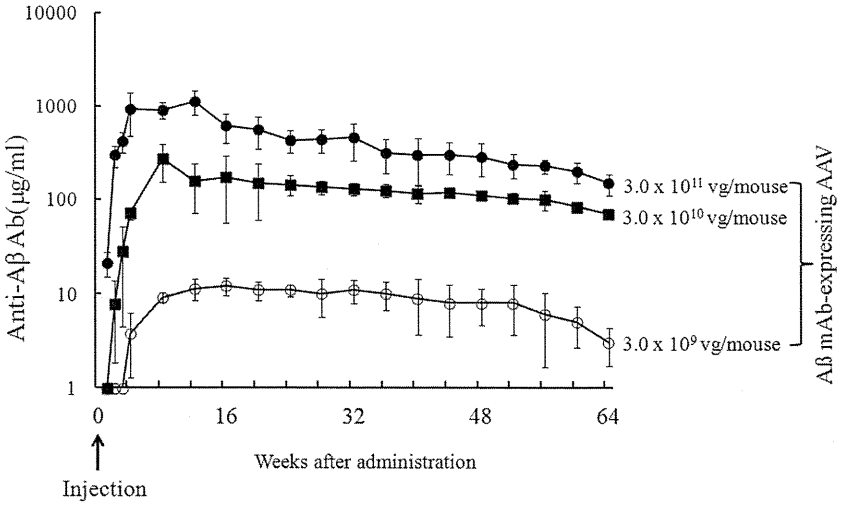

Figure 4. Kinetics of anti-Aß Ab production by mice injected with Aß mAb-expressing AAV. Normal C57BL/6 mice (n = 10/group) received a single intramuscular injection with 3.0×10^9, 3.0×10^{10}, 3.0×10^{11} vg of Aß mAb-expressing AAV or 3.0×10^{11} vg of LacZ-expressing AAV vector. The titer of IgG1 Ab binding to Aß1–42 was detected at indicated time points. Significant difference among groups received 3×10^9, 3×10^{12} and 3×10^{11} vg of Aß mAb-expressing AAV was observed from 2-week to 64-week after administration ($P<0.05$). Data are presented as mean ± SE.
doi:10.1371/journal.pone.0057606.g004

during the immunohistologic analysis of brain tissue from these animals. Aß protein containing deposits accumulated over time in the LacZ but not the Aß mAb - expressing AAV vector (Figure 6C).

Discussion

Efforts to treatment AD patients with anti-Aß Abs or through Aß peptide vaccination provided novel insights concerning the pathogenesis of AD and opened new approaches to disease therapy. In an effort to overcome limitations of earlier strategies, the current work examined the effect of delivering an Aß mAb - expressing AAV vector to Tg2576 mice (a murine model of AD). Prophylactic treatment of young (5 months) and therapeutic treatment of older (10 months) animals resulted in a significant and prolonged decrease in the amount of Aß protein accumulating in the brain (Figure 5 and 6).

The AAV vector encoded an anti-Aß mAb that bound to synthetic Aß peptides and to senile plaques present in the brains of Tg2576 mice (Figure 1 and 2). Of interest, a single 3.0×10^{10} vg dose of the Aß mAb-expressing AAV vector resulted in the production of Ab that persisted through the 64-week experimental period (Figure 4). As repeated injection of free anti-Aß mAb can have negative consequences [15], the continuous production of Ab by cells transfected in vivo may provide an ideal method for AD prophylaxis and treatment.

Previous studies investigated the utility of AAV vector for the molecular therapy of Alzheimer's disease. Those vectors encoding antigen, Ab or other factors of potential therapeutic value were examined in various animal models [20–31]. These included studies of AAV vector expressing a single-chain variable fragment (scFv) antibody against Aβ protein for AD therapy [22–26]. Those studies showed that the scFv fragment had a much shorter serum half-life than whole Ab (7–14 hrs *vs* 20 days) [32], such that the scFv fragment was more suited for intracranial delivery rather than systemic delivery [22–26]. Delivery of scFv - expressing AAV vector intracranially reduced/prevented the formation of Aβ brain plaques and improved cognitive function in AD mice [22–26], while the delivery method is likely to raise safety issues.

This study examined the effect of treating 5- or 10-month old Tg2576 mice with the Aß mAb - expressing AAV vector. Of importance, a significant decline in the concentration of Aß was found in the brains of both groups of recipient mice (monitored by ELISA and immunohistochemistry). The level of decline was similar in both groups despite the difference in when treatment was initiated (Figure 5 and 6). This may reflect the level of Aß protein being so low in young mice that the effect of therapy cannot be detected until the animals reach 15 months of age. By that time the vector had been active in both treatment groups for a sufficient period to significantly reduce the accumulation of Aß protein

Clinical trials showed that vaccination of AD patients with an Aß peptide reduced the deposition of Aß in some individuals [10]. Unfortunately, this treatment also led to the development of cerebroencephalitis in some patients, a side effect so severe that further development of this type of therapy was abandoned [11,14,33]. An alternative approach involved the intravenous administration of Abs against Aß peptide [5,8]. While effective at reducing the accumulation of Aß aggregates, the injection of anti-Aß Ab resulted in a high incidence of cerebral microhemorrhages [15]. Approximately 30% of AD patients have cerebral amyloid angiopathy (CAA)-associated microhemorrhages [34]. Shroeter et al. [35] reported that anti-Aß Ab treatment of 12-month old AD model mice resulted in a dose-dependent reduction of the occurrence of CAA after treatment. In older model mice, CAA is known to be relatively abundant [36–37]; however, the injection of a small amount of anti-Aß mAb did not increase the incidence of microhemorrhages [36–37], indicating that long-lasting expression of anti-Aß mAb by AAV vector may have some advantages in reducing the incidence of microhemorrhages. Many reports have explored the T-cell response after virus or non-virus-based vaccine against Alzheimer's. The T-cell response is very low or undetectable [38–40]. In this study, we have not explored the T-cell response, because our AAV vector expresses anti-Aβ-antibody, but not an antigen. Furthermore, we histologically evaluated the appearance of microhemorrhages and inflammation of brain in the mice treated with the Aß mAb-expressing AAV vector. No evidence of this adverse side effect was observed even in 17-month old Tg2576 mice (data not shown).

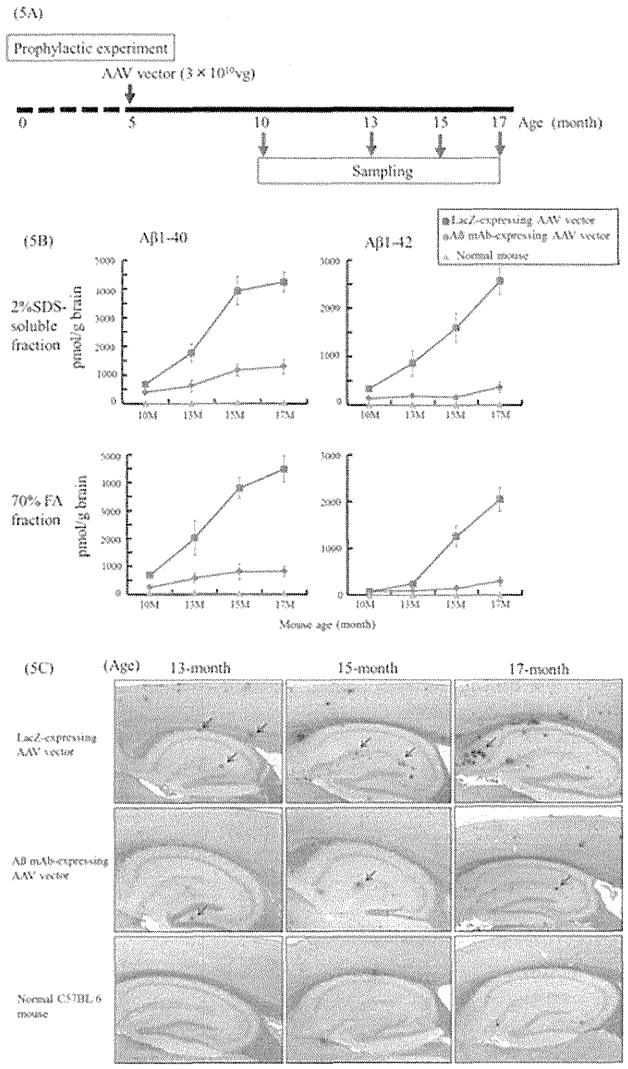

Figure 5. Prophylaxis of AD using Aß mAb-expressing AAV vector. Five-month old Tg2576 mice were injected i.m. with 3×10^{10} Aß mAb-expressing AAV. (A) Scheme of experiment. (B) The amount of Aß protein in brain extracts was determined using anti-Aß Ab-coated ELISA plates at age 10-, 13-, 15- and 17-month old (4–5 mice per time point). C57BL/6 mice were used as controls. Data are presented as mean ± SE. (C) Brain sections from Tg2576 or C57BL/6 mice were examined for Aß deposits by immunohistostaining using rabbit anti-human beta amyloid 1–42 polyclonal antibody.
doi:10.1371/journal.pone.0057606.g005

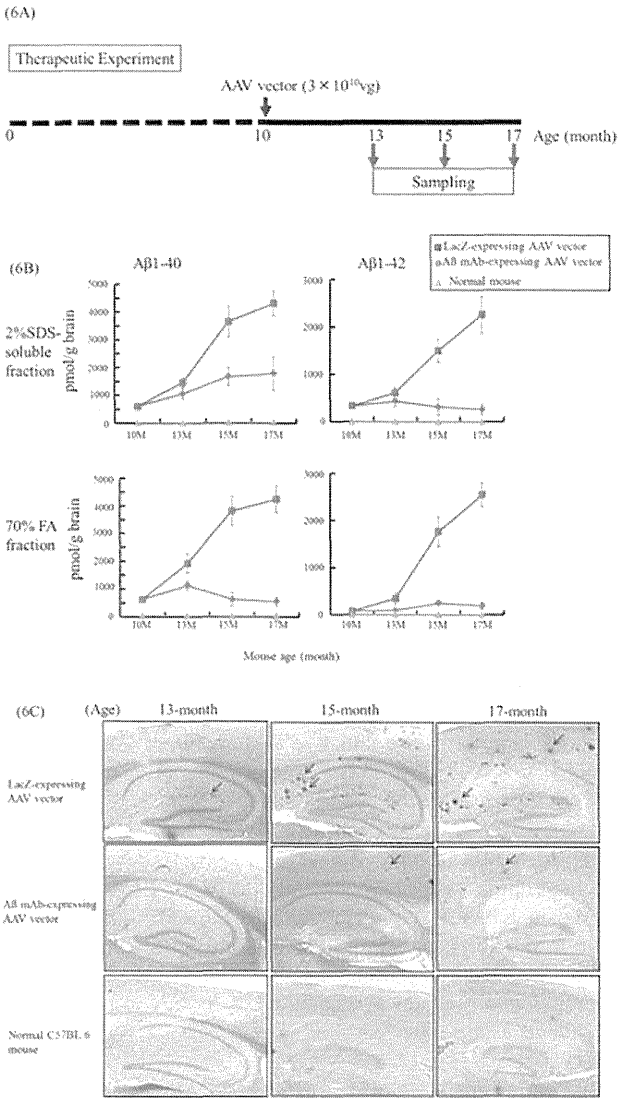

Figure 6. Therapy of AD using Aß mAb-expressing AAV vector. Tem-month old Tg2576 mice were injected i.m. with 3.0×10^{10} vg of the Aß mAb - expressing AAV vector. (A) Scheme of experiment. (B) The amount of Aß protein in brain extracts was determined using anti-Aß Ab-coated ELISA plates at age 10-, 13-, 15- and 17-month old (4–5 mice per time point). C57BL/6 mice were used as controls. Data are presented as mean ± SE. (C) Brain sections from Tg2576 or C57BL/6 mice were examined for Aß deposits by immunohistostaining using rabbit anti-human beta amyloid 1–42 polyclonal antibody.
doi:10.1371/journal.pone.0057606.g006

Recent reports suggest that mAb therapy is effective only in AD patients possessing e4/e4 proteins [12,41]. In this context, ApoE4 (+) individuals develop AD more often than ApoE4 (−) individuals [42–43]. Such observations help inform the design of trials with AAV vectors intended for human use, as it facilitates the identification of individuals at high risk for developing AD. In addition, previous studies documented that Aß oligomers are toxic to neuronal cells [44–45]. That finding is consistent with current results showing that aggregated Aß proteins are toxic to primary culture neuronal cells and that anti-Aß mAbs prevent this toxicity (Figure 3).

We hypothesize that the ongoing accumulation of Aß aggregates is responsible for widespread neuronal cell degeneration and the subsequent dementia characteristic of AD. We believe that the failure of clinical trials involving anti-Aß mAb may reflect the late initiation of such treatment as it is important to eliminate Aß oligomers during the early stages of AD. Evidence that ApoE4 and other factors can predict individuals at high risk [34] lead us to recommend clinical trials of Aß mAb - expressing AAV vector commence at an early age for prophylaxis of AD. Current results show that the production of anti-Aß mAbs persists for an extended period (Figure 4). Thus, a single early treatment may yield long term clinical benefit. Further study that includes behavioral and memory testing combined with even longer follow should help clarify the value of AAV vector mediated in the prophylaxis and/or therapy of AD treatment.

Taken together, we constructed an anti-Aβ Ab-expressing AAV vector. A single intramuscular injection of the vector generated high serum anti-Aß Ab level for up to 64 weeks, and significantly

decreased Aß levels in the brain of AD model mice treated at 5 months (prophylactic) or 10 months (therapeutic) of age. Our present results clearly demonstrated that the Aß mAb-expressing AAV vector may be of prophylactic and/or therapeutic value for AD treatment.

Materials and Methods

Ethics Statement

All animal work has been conducted according to relevant Japan and international guidelines. All experimental procedures were carried out in accordance with the Administrative Panel on Laboratory Animal Care (APLAC) protocol and the institutional guidelines set by Yokohama City University and Chyoju Medical Institute. The protocols used in this study were proved by Institutional Animal Care and Use Committee (IACUC)/Ethics committee of Yokohama City University (No. 0741, 0875 and 0974) and Chyoju Medical Institute (No. B-22).

All animal work has been conducted according to relevant U.S. and international guidelines. Specifically, all experimental procedures were carried out in accordance with the Administrative Panel on Laboratory Animal Care (APLAC) protocol and the institutional guidelines set by the Veterinary Service Center at Stanford University (Animal Welfare Assurance A3213-01 and USDA License 93-4R-00). Stanford APLAC and institutional guidelines are in compliance with the U.S. Public Health Service Policy on Humane Care and Use of Laboratory Animals. The Stanford APLAC approved the animal protocol associated with the work described in this publication.

Genes of mAbs against Aß

A hybridoma producing anti-Aß1–13 mAb (IIA2) [14] was cultured in KBM 450 medium (Kohjin Bio Co., Ltd., Saitama, Japan) in the absence of fetal bovine serum (FBS). The antibody was concentrated and partially purified from culture supernatant by ammonium sulfate precipitation and was used for the experiments as a positive control.

Aß peptide synthesis and aggregated Aß or oligomer formation

The Aß1-42 peptide used in these studies was produced by chemical synthesis (American Peptide, Sunnyvale, CA, USA). Reverse - phase high performance liquid chromatography showed that the synthesized peptide has >95% purity, and mass spectrometry analysis verified the molecular mass. Oligomer formation was done using the method described previously (Stine et al., 2003). Briefly, Aß oligomers were prepared by diluting 5 mM Aß1–42 in Me2SO to 100 µM in ice-cold cell culture supernatant (phenol red - free Ham's F-12; BioSource, CA, USA), immediately vortexing for 30 s, and incubating at 4°C, room temperature or 37°C for 24 h. The aggregated Aß or oligomer solution was used for the Western blotting analysis, as well as cytotoxic tests of neural cells.

Construction of an expression vector for the anti-Aß mAb gene

Total RNA was extracted from a hybridoma producing anti-Aß1–13 mAb (IIA2) [14] using TRIzol Reagent (Gibco BRL, Grand Island, NY, USA). Full-length heavy (H) chain and light (L) chain cDNA was transcribed with 5′-RACE primer and 3′-RACE primer using BD SMART RACE cDNA Amplification Kit (Clontech, Mountain View, CA, USA) according to the manufacturer's instructions. H chain cDNA was amplified with sense primer (5′ CGG GGT ACC ATG GGC AGG CTT ACT TCT TC 3′) and antisense primer (5′ CCC AAG CTT TTT ACC AGG AGA GTG GGA GA 3′). L chain cDNA was amplified with sense primer (5′ CCG GAA TTC ATG GAG ACA GAC ACA CTC CT 3′) and antisense primer (5′ ATA AGA ATG CGG CCG CA G TCG ACG CTA ACA CTC ATT CCT GTT GA 3′). The Furin 2A fragment [46–47] from the foot and mouth disease virus was synthesized with complementary oligo (5′ CCC AAG CTT CGC GCC AAG CGC GCC CCC GT 3′ and 5′ CCG GAA TTC GGG GCC GGG GTT GGA CTC CA 3′). The H chain–Furin 2A–L chain fusion fragment was subcloned into proviral plasmid pW1 controlled by the CMV promoter. The AAV vectors were prepared by the previously described three - plasmid transfection adenovirus-free protocol [16,48]. Briefly, 60% confluent human embryonic kidney 293 (HEK293) cells were maintained in Dulbecco's modified Eagle's medium – nutrient mixture F-12 (1:1) (DMEM/F-12; GIBCOBRL, New York, NY) supplemented with 10% fetal bovine serum (FBS). Cells were cultured at 37°C in an atmosphere of 5% CO2 in air. Subconfluent HEK293 cells were co-transfected by the calcium phosphate co-precipitation method with the AAV shuttle plasmid pW1 (containing LacZ or antibody heavy chain-F2A-light chain), the AAV-1 chimeric helper plasmid p1RepCap (provided by Dr. James M. Wilson, University of Pennsylvania, Philadelphia, PA, USA), and the adenoviral helper plasmid pAdeno (provided by Avigen, Inc., Alamada, CA, USA). After 48 h, the cells were harvested and lysed in Tris buffer (10 mM Tris-HCl, 150 mM NaCl, pH 8.0) by three cycles of freezing and thawing. One round of sucrose precipitation and two rounds of CsCl density-gradient ultracentrifugation were sufficient to isolate the AAV vector from the lysates. The vector titer was determined by quantitative PCR and presented as vg.

Western blot analysis

To confirm the expression of the Ab proteins, HEK293 cells were transduced with the AAV vector encoding the mAb genes (Aß mAb-expressing vector) in a 6-well plate. After transduction of AAV vector for 2 h, the cells were washed twice with PBS and cultured with Ex-CELL CD CHO serum-free medium (Life Technologies Japan Ltd, Tokyo, Japan) for another 2 days. Then, antibody protein was detected in culture supernatant and cell lysates with Western blot. The cells were washed with PBS and lysed with 0.1 M Tris-HCl (pH 7.8) and 0.125% Nonidet P-40 2 days after transduction. The cell lysates were mixed with an equal volume of 2× SDS buffer (125 mM Tris-HCl [pH 6.8], 4% SDS) with 100 mM of DTT (reducing condition) or without DTT (non-reducing condition) and boiled for 10 min. The cell lysates were loaded on an 8% polyacrylamide gel and transferred to a Hybond ECL nitrocellulose membrane. After rinsing with PBS, the membrane was probed with HRP-labeled goat anti-mouse IgG1 or IgκAbs (Ig; ICN Pharmaceuticals Inc., Solon, OH, USA). The protein was detected using the ECL Plus Western Blotting Detection System (Amersham Pharmacia Biotech, Uppsala, Sweden).

Animals and administration

Heterozygous Tg2576 mice were obtained from Taconic Farms Inc. (Germantown, NY, USA) [14]. Normal C57BL/6 female mice were purchased from Japan SLC Inc. (Hamamatsu, Japan). The mice were housed in the animal centers located at Yokohama City University and Chyoju Medical Institute, and maintained on a 12-h day–night cycle. Five-month and 10-month old mice were used for prophylactic and therapeutic experiments, respectively. The mice were received a single injection in quadriceps muscles

with a dose of 3.0×10^{10} vg of the Aß mAb-expressing vector. We used 20–25 mice in each group. The mice for prophylactic experiments were sacrificed 5, 8, 10 and 12 months after Aß mAb - expressing vector administration and the mice for therapeutic experiments were sacrificed 0, 3, 5 and 7 months after Aß mAb-expressing vector administration. To explore the magnitude and duration of antibody expression, we injected 3.0×10^{9}, 3.0×10^{10} and 3.0×10^{11} vg of Aß mAb-expressing vector or 3.0×10^{11} vg of AAV vector expressing LacZ gene (LacZ-expressing vector) to mouse quadriceps muscles, and blood was collected at indicated time points for Aβ-specific antibody detection. The animal experiments were approved by the Animal Ethical Committees of Yokohama City University School of Medicine and and Chyoju Medical Institute.

Enzyme-linked immunosorbent assay (ELISA) for Ab titers

ELISA was performed as described previously [14]. Briefly, 96-well microtiter plates were coated with 40 μg/ml of Aß1-42 peptide in 0.15 M phosphate-buffered saline (PBS). The wells were rinsed with 0.15 M PBS and then blocked with 3% FBS in 0.15 M PBS for 1 h. Appropriately diluted mAb as well as the serum from AAV vector-administered mouse were incubated on antigen-coated plates for 6 h at 4°C. Then, wells were rinsed with 0.15 M PBS and the bound Abs were detected using HRP-coupled goat anti-mouse IgG1 (Pierce Chemical Co., Rockford, IL, USA). We detected IgG1 titer rather than total IgG titer, because transgene of the AAV vector was isolated from the mouse IgG1-secreting hybridoma (IIA2). The anti-Aß1–13 mAb (IIA2) purified from the hybridoma was used as a standard control.

Brain sample preparation for histochemical studies

Brains were removed and divided sagittally along the interhemispheric fissure. The right hemisphere was dissected from the cerebella. Brain samples were snap frozen in large test tubes containing n-hexane, immersed in a dry ice/acetone mixture, and stored at −80°C until processing. The left hemisphere was fixed with formalin and then embedded in paraffin for histochemical studies. To test whether Aß mAb-expressing vector-produced antibody can be used for immunostaining against human Aß, Culture supernatant of Aß mAb - expressing vector-transduced HEK293 cells was used as a first antibody and HRP-Goat ant-mouse IgG1 antibody used as a second antibody. Rabbit anti-human beta amyloid (1–42) antibody (Genetex, Inc., Irvine, CA) and mAb purified from hybridoma IIA2 were used as controls. Paraffin samples from AAV vector administrated mice were stained with the rabbit anti-human beta amyloid (1–42) antibody.

ELISA to measure Aß protein levels in the brain

The frozen left cerebra were obtained from each mouse and homogenized with a homogenizer in Tris-buffered saline buffer (TBS, 50 mM Tris, 150 mM NaCl, pH 7.6) containing protease inhibitor cocktail (Nacalai, San Diego, CA, USA) with 20 μg/ml pepstatin A, then centrifuged at 100,000 *g* for 1 h at 4°C using an Optima TLX ultracentrifuge (Beckman Coulter Inc., Fullerton, CA, USA). The pellets were homogenized in TBS buffer containing 2% SDS and protease inhibitor cocktail (Nacalai, San Diego, CA, USA) following incubation at 37°C for 15 min. Then the solution was centrifuged again at 100,000 *g* for 1 h at 25°C. The supernatant and pellet correspond to the soluble (2% SDS soluble fraction) and insoluble fraction, respectively.

The insoluble fraction was washed, then extracted again with 70% formic acid and centrifuged at 100,000 *g* for 1 h. The supernatants of 70% formic acid extracts were neutralized with 1 M Tris-HCl, pH 8.0 at a dilution of 1:20 (70% FA fraction). The dissolved samples of Aß1–42 or Aß1–40 protein were quantified using Human Amyloid ß (N3pE-42) Kit and Human Amyloid ß (N3pE-40) assay kit, respectively (IBL Co., Ltd., Gunma, Japan). The values obtained were corrected with the wet weight of each brain hemisphere sample and expressed as pmol/g brain.

Cytotoxicity inhibition test by Abs from AAV-transduced cells using primary culture hippocampal cell

Hippocampal cells were collected from 15-day-old fetal mouse brains and gently minced. The samples were incubated at 37°C for 5 min in 9 ml of 0.15 M PBS and 1 ml of 2.5% trypsin, followed by addition of 1 ml 0.5% trypsin inhibitor on ice. The cells were washed twice with 0.15 M PBS and resuspended in media stock (MS) supplemented with 20% FBS, 10 ng/ml epidermal growth factor, 50 IU/ml penicillin, and 50 μg/mL streptomycin. MS is composed of modified Eagle's medium supplemented with 2 mM glutamine and 20 mM glucose [49].

We reacted 5.0×10^{4} primary culture hippocampal cells in 100 μl MS per well with each concentration of aggregated Aß solution with or without Aß mAb - expressing vector-transduced culture supernatant in a humidified atmosphere (37°C, 5% CO2). After 6 and 24 h incubation, 10 μL 3-[4,5-dimethylthiazol-2-yl]-2,5-diphenyl tetrazolium bromide (MTT) reagent (final concentration 0.5 mg/ml) was added to each well. The microplate was incubated for 4 h in a humidified atmosphere [50]. Then, 100 μl of the solubilization solution was added into each well to solubilize the purple formazan crystals, and the absorbance of the samples was measured using an ELISA microplate reader [51].

Data analysis

All values were expressed as the mean ± standard error (SE). Statistical analysis (Student's t-test) of the experimental data and controls was conducted using two-way factorial analysis of variance. Significance was defined as $P<0.05$ for statistical analysis using all time points in each group.

Acknowledgments

We would like to thank Ms. M. Kawano, Mr. T. Kanesaka for their technical assistances. This work was supported in part by a grant-in-aid for the Ministry of Education, Science, Sports, Culture of Japan, and the Ministry of Health and Welfare of Japan.

Author Contributions

Conceived and designed the experiments: K. Ozawa K. Okuda. Performed the experiments: MS SA TT. Analyzed the data: KS DMK. Contributed reagents/materials/analysis tools: MO HM. Wrote the paper: MS K. Okuda.

References

1. De Felice FG, Wu D, Lambert MP, Fernandez SJ, Velasco PT, et al. (2008) Alzheimer's disease-type neuronal tau hyperphosphorylation induced by A beta oligomers. Neurobiol Aging. 29: 1334–1347.
2. Zhang YW, Thompson R, Zhang H, Xu H (2011) APP processing in Alzheimer's disease. Mol Brain. 4: 3.
3. Schenk D, Barbour R, Dunn W, Gordon G, Grajeda H, et al. (1999) Immunization with amyloid-beta attenuates Alzheimer-disease-like pathology in the PDAPP mouse. Nature. 400: 173–177.
4. Morgan D, Diamond DM, Gottschall PE, Ugen KE, Dickey C, et al. (2000) A beta peptide vaccination prevents memory loss in an animal model of Alzheimer's disease. Nature. 408: 982–985.

5. Nicoll JA, Wilkinson D, Holmes C, Steart P, Markham H, et al. (2003) Neuropathology of human Alzheimer disease after immunization with amyloid-beta peptide: a case report. Nat Med. 9: 448–452.
6. Ferrer I, Boada Rovira M, Sanchez Guerra ML, Rey MJ, Costa-Jussa F (2004) Neuropathology and pathogenesis of encephalitis following amyloid-beta immunization in Alzheimer's disease. Brain Pathol. 14: 11–20.
7. Check E (2002) Nerve inflammation halts trial for Alzheimer's drug. Nature. 415: 462.
8. Orgogozo JM, Gilman S, Dartigues JF, Laurent B, Puel M, et al. (2003) Subacute meningoencephalitis in a subset of patients with AD after Abeta42 immunization. Neurology. 61: 46–54.
9. Nicoll JA, Barton E, Boche D, Neal JW, Ferrer I, et al. (2006) Abeta species removal after abeta42 immunization. J Neuropathol Exp Neurol. 65: 1040–1048.
10. Holmes C, Boche D, Wilkinson D, Yadegarfar G, Hopkins V, et al. (2008) Long-term effects of Abeta42 immunisation in Alzheimer's disease: follow-up of a randomised, placebo-controlled phase I trial. Lancet. 372: 216–223.
11. DeMattos RB, Bales KR, Cummins DJ, Dodart JC, Paul SM, et al. (2001) Peripheral anti-A beta antibody alters CNS and plasma A beta clearance and decreases brain A beta burden in a mouse model of Alzheimer's disease. Proc Natl Acad Sci U S A. 98: 8850–8855.
12. Salloway S, Sperling R, Gilman S, Fox NC, Blennow K, et al. (2009) A phase 2 multiple ascending dose trial of bapineuzumab in mild to moderate Alzheimer disease. Neurology. 73: 2061–2070.
13. Black RS, Sperling RA, Safirstein B, Motter RN, Pallay A, et al. (2010) A single ascending dose study of bapineuzumab in patients with Alzheimer disease. Alzheimer Dis Assoc Disord. 24: 198–203.
14. Tamura Y, Hamajima K, Matsui K, Yanoma S, Narita M, et al. (2005) The F(ab)'2 fragment of an Abeta-specific monoclonal antibody reduces Abeta deposits in the brain. Neurobiol Dis. 20: 541–549.
15. Pfeifer M, Boncristiano S, Bondolfi L, Stalder A, Deller T, et al. (2002) Cerebral hemorrhage after passive anti-Abeta immunotherapy. Science. 298: 1379.
16. Xin KQ, Urabe M, Yang J, Nomiyama K, Mizukami H, et al. (2001) A novel recombinant adeno-associated virus vaccine induces a long-term humoral immune response to human immunodeficiency virus. Hum Gene Ther. 12: 1047–1061.
17. Stine WB Jr, Dahlgren KN, Krafft GA, LaDu MJ (2003) In vitro characterization of conditions for amyloid-beta peptide oligomerization and fibrillogenesis. J Biol Chem. 278: 11612–11622.
18. Brantly ML, Spencer LT, Humphries M, Conlon TJ, Spencer CT, et al. (2006) Phase I trial of intramuscular injection of a recombinant adeno-associated virus serotype 2 alphal-antitrypsin (AAT) vector in AAT-deficient adults. Hum Gene Ther. 17: 1177–1186.
19. Jiang H, Pierce GF, Ozelo MC, de Paula EV, Vargas JA, et al. (2006) Evidence of multiyear factor IX expression by AAV-mediated gene transfer to skeletal muscle in an individual with severe hemophilia B. Mol Ther. 14: 452–455.
20. Hara H, Monsonego A, Yuasa K, Adachi K, Xiao X, et al. (2004) Development of a safe oral Abeta vaccine using recombinant adeno-associated virus vector for Alzheimer's disease. J Alzheimers Dis. 6: 483–488.
21. Mouri A, Noda Y, Hara H, Mizoguchi H, Tabira T, et al. (2007) Oral vaccination with a viral vector containing Abeta cDNA attenuates age-related Abeta accumulation and memory deficits without causing inflammation in a mouse Alzheimer model. FASEB J. 21: 2135–2148.
22. Fukuchi K, Tahara K, Kim HD, Maxwell JA, Lewis TL, et al. (2006) Anti-Abeta single-chain antibody delivery via adeno-associated virus for treatment of Alzheimer's disease. Neurobiol Dis. 23: 502–511.
23. Levites Y, Jansen K, Smithson LA, Dakin R, Holloway VM, et al. (2006) Intracranial adeno-associated virus-mediated delivery of anti-pan amyloid beta, amyloid beta40, and amyloid beta42 single-chain variable fragments attenuates plaque pathology in amyloid precursor protein mice. J Neurosci. 26: 11923–11928.
24. Sudol KL, Mastrangelo MA, Narrow WC, Frazer ME, Levites YR, et al. (2009) Generating differentially targeted amyloid-beta specific intrabodies as a passive vaccination strategy for Alzheimer's disease. Mol Ther. 17: 2031–2040.
25. Ryan DA, Mastrangelo MA, Narrow WC, Sullivan MA, Federoff HJ, et al. (2010) Abeta-directed single-chain antibody delivery via a serotype-1 AAV vector improves learning behavior and pathology in Alzheimer's disease mice. Mol Ther. 18: 1471–1481.
26. Kou J, Kim H, Pattanayak A, Song M, Lim JE, et al. (2011) Anti-Amyloid-beta Single-Chain Antibody Brain Delivery Via AAV Reduces Amyloid Load But May Increase Cerebral Hemorrhages in an Alzheimer's Disease Mouse Model. J Alzheimers Dis. 27: 23–38.
27. Feng X, Eide FF, Jiang H, Reder AT (2004) Adeno-associated viral vector-mediated ApoE expression in Alzheimer's disease mice: low CNS immune response, long-term expression, and astrocyte specificity. Front Biosci. 9: 1540–1546.
28. Carty NC, Nash K, Lee D, Mercer M, Gottschall PE, et al. (2008) Adeno-associated viral (AAV) serotype 5 vector mediated gene delivery of endothelin-converting enzyme reduces Abeta deposits in APP + PS1 transgenic mice. Mol Ther. 16: 1580–1586.
29. Liu Y, Studzinski C, Beckett T, Guan H, Hersh MA, et al. (2009) Expression of neprilysin in skeletal muscle reduces amyloid burden in a transgenic mouse model of Alzheimer disease. Mol Ther. 17: 1381–1386.
30. Mandel RJ (2010) CERE-110, an adeno-associated virus-based gene delivery vector expressing human nerve growth factor for the treatment of Alzheimer's disease. Curr Opin Mol Ther. 12: 240–247.
31. Chu J, Giannopoulos PF, Ceballos-Diaz C, Golde TE, Pratico D (2012) Adeno-associated virus-mediated brain delivery of 5-lipoxygenase modulates the AD-like phenotype of APP mice. Mol Neurodegener. 7: 1.
32. Fitch JC, Rollins S, Matis L, Alford B, Aranki S, et al. (1999) Pharmacology and biological efficacy of a recombinant, humanized, single-chain antibody C5 complement inhibitor in patients undergoing coronary artery bypass graft surgery with cardiopulmonary bypass. Circulation. 100: 2499–2506.
33. Bard F, Cannon C, Barbour R, Burke RL, Games D, et al. (2000) Peripherally administered antibodies against amyloid beta-peptide enter the central nervous system and reduce pathology in a mouse model of Alzheimer disease. Nat Med. 6: 916–919.
34. McCarron MO, Nicoll JA (2004) Cerebral amyloid angiopathy and thrombolysis-related intracerebral haemorrhage. Lancet Neurol. 3: 484–492.
35. Schroeter S, Khan K, Barbour R, Doan M, Chen M, et al. (2008) Immunotherapy reduces vascular amyloid-beta in PDAPP mice. J Neurosci. 28: 6787–6793.
36. Wilcock DM, Alamed J, Gottschall PE, Grimm J, Rosenthal A, et al. (2006) Deglycosylated anti-amyloid-beta antibodies eliminate cognitive deficits and reduce parenchymal amyloid with minimal vascular consequences in aged amyloid precursor protein transgenic mice. J Neurosci. 26: 5340–5346.
37. Karlnoski RA, Rosenthal A, Alamed J, Ronan V, Gordon MN, et al. (2008) Deglycosylated anti-Abeta antibody dose-response effects on pathology and memory in APP transgenic mice. J Neuroimmune Pharmacol. 3: 187–197.
38. Chackerian B, Rangel M, Hunter Z, Peabody DS (2006) Virus and virus-like particle-based immunogens for Alzheimer's disease induce antibody responses against amyloid-beta without concomitant T cell responses. Vaccine. 24: 6321–6331.
39. Nikolic WV, Bai Y, Obregon D, Hou H, Mori T, et al. (2007) Transcutaneous beta-amyloid immunization reduces cerebral beta-amyloid deposits without T cell infiltration and microhemorrhage. Proc Natl Acad Sci U S A. 104: 2507–2512.
40. Okura Y, Miyakoshi A, Kohyama K, Park IK, Staufenbiel M, et al. (2006) Nonviral Abeta DNA vaccine therapy against Alzheimer's disease: long-term effects and safety. Proc Natl Acad Sci U S A. 103: 9619–9624.
41. Farlow MR (2010) Should the ApoE genotype be a covariate for clinical trials in Alzheimer disease? Alzheimers Res Ther. 2: 15.
42. Dafnis I, Stratikos E, Tzinia A, Tsilibary EC, Zannis VI, et al. (2010) An apolipoprotein E4 fragment can promote intracellular accumulation of amyloid peptide beta 42. J Neurochem. 115: 873–884.
43. Fleisher AS, Chen K, Liu X, Ayutyanont N, Roontiva A, et al. (2012) Apolipoprotein E epsilon4 and age effects on florbetapir positron emission tomography in healthy aging and Alzheimer disease. Neurobiol Aging.
44. Yankner BA, Duffy LK, Kirschner DA (1990) Neurotrophic and neurotoxic effects of amyloid beta protein: reversal by tachykinin neuropeptides. Science. 250: 279–282.
45. Takuma H, Teraoka R, Mori H, Tomiyama T (2008) Amyloid-beta E22Delta variant induces synaptic alteration in mouse hippocampal slices. Neuroreport. 19: 615–619.
46. Fang J, Qian JJ, Yi S, Harding TC, Tu GH, et al. (2005) Stable antibody expression at therapeutic levels using the 2A peptide. Nat Biotechnol. 23: 584–590.
47. Shoji M, Yoshizaki S, Mizuguchi H, Okuda K, Shimada M (2012) Immunogenic comparison of chimeric adenovirus 5/35 vector carrying optimized human immunodeficiency virus clade C genes and various promoters. PLoS One. 7: e30302.
48. Okada T, Nomoto T, Yoshioka T, Nonaka-Sarukawa M, Ito T, et al. (2005) Large-scale production of recombinant viruses by use of a large culture vessel with active gassing. Hum Gene Ther. 16: 1212–1218.
49. Akiyama H, Mori H, Saido T, Kondo H, Ikeda K, et al. (1999) Occurrence of the diffuse amyloid beta-protein (Abeta) deposits with numerous Abeta-containing glial cells in the cerebral cortex of patients with Alzheimer's disease. Glia. 25: 324–331.
50. Berridge MV, Herst PM, Tan AS (2005) Tetrazolium dyes as tools in cell biology: new insights into their cellular reduction. Biotechnol Annu Rev. 11: 127–152.
51. Hsiao K, Chapman P, Nilsen S, Eckman C, Harigaya Y, et al. (1996) Correlative memory deficits, Abeta elevation, and amyloid plaques in transgenic mice. Science. 274: 99–102.

Biochemical and Biophysical Research Communications 438 (2013) 84–89

Contents lists available at SciVerse ScienceDirect

Biochemical and Biophysical Research Communications

journal homepage: www.elsevier.com/locate/ybbrc

CD19 target-engineered T-cells accumulate at tumor lesions in human B-cell lymphoma xenograft mouse models

Tomonori Tsukahara [a,c,*], Ken Ohmine [b,c], Chihiro Yamamoto [b], Ryosuke Uchibori [a,c], Hiroyuki Ido [c], Takeshi Teruya [c], Masashi Urabe [a], Hiroaki Mizukami [a], Akihiro Kume [a], Masataka Nakamura [d], Junichi Mineno [e], Kazutoh Takesako [e], Isabelle Riviere [f], Michel Sadelain [f], Renier Brentjens [f], Keiya Ozawa [a,b,c]

[a] Division of Genetic Therapeutics, Center for Molecular Medicine, Jichi Medical University, Japan
[b] Division of Hematology, Department of Medicine, Jichi Medical University, Japan
[c] Division of Immuno-Gene & Cell Therapy (Takara Bio), Jichi Medical University, Japan
[d] Human Gene Sciences Center, Tokyo Medical and Dental University, Japan
[e] Center for Cell and Gene Therapy, Takara Bio Inc., Japan
[f] Department of Medicine, Memorial Sloan Kettering Cancer Center, USA

ARTICLE INFO

Article history:
Received 8 July 2013
Available online 17 July 2013

Keywords:
Adoptive T-cell therapy
CD19
Tumor targeting
B-cell lymphoma
Chimeric antigen receptor

ABSTRACT

Adoptive T-cell therapy with CD19-specific chimeric antigen receptors (CARs) is promising for treatment of advanced B-cell malignancies. Tumor targeting of CAR-modified T-cells is likely to contribute therapeutic potency; therefore we examined the relationship between the ability of CD19-specific CAR (CD19-CAR)-transduced T-cells to accumulate at $CD19^+$ tumor lesions, and their ability to provide anti-tumor effects in xenograft mouse models. Normal human peripheral blood lymphocytes, activated with immobilized RetroNectin and anti-CD3 antibodies, were transduced with retroviral vectors that encode CD19-CAR. Expanded CD19-CAR T-cells with a high transgene expression level of about 75% produced IL-2 and IFN-γ in response to CD19, and lysed both Raji and Daudi $CD19^+$ human B-cell lymphoma cell lines. Furthermore, these cells efficiently accumulated at Raji tumor lesions where they suppressed tumor progression and prolonged survival in tumor-bearing $Rag2^{-/-}\gamma c^{-/-}$ immunodeficient mice compared to control cohorts. These results show that the ability of CD19-CAR T-cells to home in on tumor lesions is pivotal for their anti-tumor effects in our xenograft models, and therefore may enhance the efficacy of adoptive T-cell therapy for refractory B-cell lymphoma.

1. Introduction

Chimeric antigen receptor (CAR)-based T-cell therapy is a promising approach to targeted cancer immunotherapy. CARs are hybrid proteins consisting of an extracellular single chain fragment of variable region (scFv) fused to intracellular lymphocyte signaling domains CD28 or 4-1BB (CD137), coupled with CD3ζ, to mediate T-cell activation. This particular configuration of CARs is widely used in current preclinical and clinical studies [1]. Independent of the human leukocyte antigen system, CAR-transduced T-cells can directly recognize and kill tumor cells that express specific cell surface antigens.

CD19 antigen is an attractive target for CAR-based T-cell therapy since it is a B-cell lineage-specific surface molecule, which is expressed on normal and most malignant B-cells but not on hematopoietic stem cells [2]. Preclinical studies have demonstrated that CD19-specific CAR (CD19-CAR) T-cells eliminated $CD19^+$ B-cell malignancies [3–5]. Recent phase I clinical trials using CD19-CAR T-cells have been shown to be safe and exhibit impressive anti-tumor effects for advanced $CD19^+$ chronic lymphocytic leukemia (CLL), acute lymphoblastic leukemia (ALL), and B-cell lymphoma patients [6–11]. However, the optimal CAR-based T-cell therapy for maximizing therapeutic potency is yet to be realized.

Both persistence and tumor targeting of adoptive transferred CAR-modified T-cells are likely to contribute to therapeutic potency. Preclinical and early clinical trial results have shown that persistence of CD19-CAR T-cells *in vivo* was correlated with anti-tumor effects for B-cell malignancies [4,5,12]. Thus, CAR designs

Abbreviations: CAR, chimeric antigen receptor; CD19-CAR T-cells, CD19-specific CAR-transduced T-cells.

* Corresponding author at: Division of Genetic Therapeutics, Center for Molecular Medicine, Jichi Medical University, 3311-1 Yakushiji, Shimotsuke, Tochigi 329-0498, Japan. Fax: +81 285 44 8675.
E-mail address: ttsukahara@jichi.ac.jp (T. Tsukahara).

0006-291X/$ - see front matter © 2013 Elsevier Inc. All rights reserved.
http://dx.doi.org/10.1016/j.bbrc.2013.07.030

which involve a signaling feature, that activates and prolongs T-cell survival *in vivo*, have been extensively pursued [13–16]. In contrast, much less is known regarding the correlation between the anti-tumor effects of CD19-CAR T-cells and their tumor targeting ability.

In the present study, we generated large numbers of primary T-cells that expressed CD19-CAR with a CD28 signaling domain. These expanded T-cells exhibited CD19-dependent redirected effector functions *in vitro*. We also observed that they accumulated at the site of tumors and exhibited anti-tumor effects at these sites in human B-cell lymphoma xenograft immunodeficient mice. Our results show that efficient accumulation at tumors of CD19-CAR T-cells can enhance CAR-based T-cell therapy for B-cell lymphoma.

2. Materials and methods

2.1. Plasmids

The gamma retroviral vector SFG-1928z that encodes CD19-specific scFv fused to CD28- and CD3ζ intracellular signal domains has been described [3] (Fig. 1A). A luciferase expression plasmid pEF-Luc was generated by ligating the luciferase gene from pGL3 (Promega, Madison, WI) into a pEF-PGKneo vector containing the EF1α promoter and Neomycin resistance gene cassette [17].

2.2. Peripheral blood lymphocytes and cell lines

Peripheral blood lymphocytes (PBLs) from three healthy donors were obtained with the approval of the Jichi Medical University Institutional Review Board, and written consent of each donor.

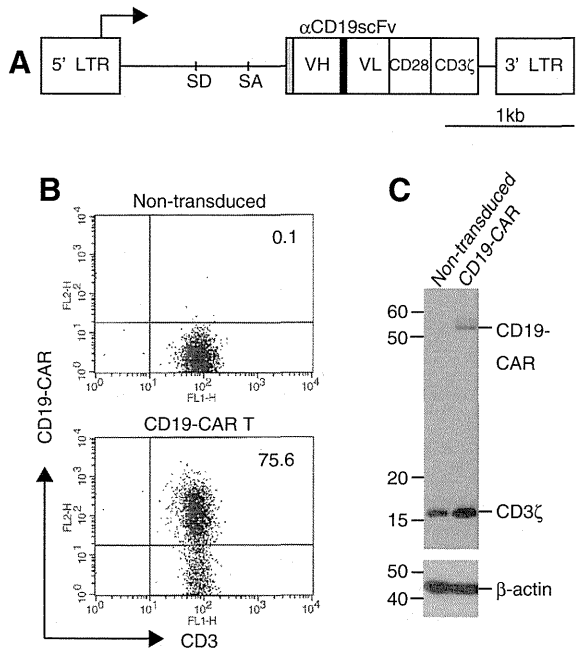

Fig. 1. Generation of CD19-CAR modified T-cells using RetroNectin/anti-CD3 stimulation. (A) Schematic structure of SFG-1928z retroviral vector. VH and VL: variable heavy- and light chain; SD: splice donor; SA: splice acceptor; LTR: long terminal repeat; Gray box: CD8α signal peptide; Black box: $(GGGGS)_3$ linker. PBLs were stimulated with RetroNectin/anti-CD3 and transduced twice with SFG-1928z retroviral vectors. They were propagated on $CD19^+$ feeder cells. (B) Surface expression of CD19-CAR on transduced or non-transduced T-cells was examined by flow cytometry. All numbers show the percentages of $CD3^+$ $CD19\text{-}CAR^+$ populations. Representative data was shown in three independent experiments. (C) CD19-CAR expression in cell lysates from transduced T-cells or the control non-transduced T-cells was detected by Western blotting with anti-CD3ζ; β-actin is a loading control.

PBLs were cultured with X-VIVO 15 (Takara Bio, Shiga, Japan), supplemented with 5% human AB serum (NOVA Biologics, Oceanside, CA) and 1 nanomolar recombinant human interleukin-2 (IL-2) (Life technologies, Carlsbad, CA). The retrovirus packaging cells PG13 [18] and mouse fibroblast NIH3T3 cells that expresses human CD19 (3T3/CD19) [19] were cultured with DMEM, supplemented with 10% FBS. Human Burkitt lymphoma cell lines Raji and Daudi (Health Science Research Resources Bank, Osaka, Japan) were maintained in RPMI1640 supplemented with 10% FBS. Raji cells expressing luciferase (Raji/Luc) were established by transfection with the pEF-Luc plasmid, followed by G418 selection.

2.3. Retroviral transduction and T-cell expansion

For retroviral transduction, PBLs were stimulated with 20 μg/ml of immobilized RetroNectin (Takara Bio) and 10 μg/ml anti-CD3ε antibodies (R&D Systems, Minneapolis, MN) for 3 days and transduced with retroviral particles using a preloading method [20]. Briefly, PG13 viral producer cells were established by stable transduction of SFG-1928z retroviral vectors (Fig. 1A). RetroNectin-coated plates were loaded with retroviral particles obtained from the PG13 cells, and centrifuged (1000g, 2 h, 32 °C). Stimulated PBMCs were added to the preloaded plates, and incubated overnight. The procedure was repeated on the next day. For selective *ex vivo* expansion, transduced T-cells were co-cultured with γ-irradiated (50 Gy) 3T3/CD19 cells at 1:1 ratio. On days 5 and 10, the 3T3/CD19 cells were added to the T-cell cultures.

2.4. Flow cytometry

We analyzed cell surface expression of CD19-CAR on transduced T-cells by flow cytometry using a BD LSR with CellQuest software (BD Biosciences, San Jose, CA). Antibodies used for CD19-CAR detection were biotin goat anti-mouse F (ab′), PE Streptavidin (Jackson Immunoresearch, West Grove, PA), and FITC anti-human CD3 (Biolegend, San Jose, CA). Isotype-matched antibodies were used as controls.

2.5. Western blotting

CD19-CAR cellular protein expression was examined by Western blotting. Cell lysate prepared from CD19-CAR T-cells was separated on 12% polyacrylamide gels and then transferred to polyvinylidene difluoride membranes (Millipore, Billerica, MA). The membranes were incubated with a mouse monoclonal anti-human CD3ζ antibody (BD Biosciences) or a rabbit anti-human β-actin antibody (Cell Signaling, Danvers, MA) as a control, followed by anti-mouse immunoglobulin conjugated with horseradish peroxidase. Proteins recognized by antibodies were visualized with an enhanced chemiluminescent detection system (GE Healthcare, Buckinghamshire, UK).

2.6. ELISA

Supernatants from the duplicate wells of co-cultures of 3T3/CD19 cells with CD19-CAR T-cells at 1:1 ratio were harvested after 48 h incubation. Human IL-2 and IFN-γ levels in supernatants were measured by ELISA kits (Biolegend).

2.7. Cell lytic activity

Cell lytic activity of CD19-CAR T-cells was examined by standard 4-h chromium release assays [21].

2.8. Mouse tumor model

To determine if modified T-cells accumulated at tumor lesions *in vivo*, 10- to 12-week-old Balb/c Rag2$^{-/-}\gamma c^{-/-}$ (Rag2$^{-}/\gamma^{-}$) immunodeficient mice [22–24] were injected subcutaneously with 5×10^6 Raji/Luc cells. Two weeks after inoculation, 10^7 CD19-CAR T-cells were injected intravenously into tumor-bearing mice. Tumors were removed 24 h after T-cell infusion, and analyzed by immunohistochemistry with an anti-human CD3 antibody (Dako, Glostrup, Denmark). The localization of human CD3$^+$ T-cells was examined using a BX50 microscope (Olympus, Tokyo, Japan). To evaluate accumulation at tumor sites of CAR-modified T-cells and their anti-tumor effects, Rag2$^{-}/\gamma^{-}$ mice injected intravenously with 5×10^4 Raji/Luc cells on day 0, were adoptively transferred with a single intravenous infusion of 10^7 CD19-CAR T-cells on day 3. To monitor the progression of Raji/Luc cells *in vivo*, the substrate of luciferase, D-luciferin was injected intraperitonealy into mice (75 mg/kg body weight), and bioluminescence imaging was performed using an IVIS imaging system (Xenogen, Hopkinton, MA) with Living Image software (Xenogen). In this therapeutic experiment, accumulations at tumor lesions of CD19-CAR T-cells were determined by immunohistochemistry as described above. All mouse experiments were carried out in a humane manner after receiving approval from the Institutional Animal Experiment Committee of Jichi Medical University.

2.9. Statistics

Student's *t* test was used to evaluate *in vitro* experimental differences. Survival data was assessed by the log-rank test. GraphPad Prism 5 (GraphPad Software, San Diego, CA) was used for the statistical calculations. $p < 0.05$ was considered statistically significant.

3. Results and discussion

3.1. Generation of CD19-CAR T-cells and transgene expression

To generate CD19-CAR T-cells, we utilized RetroNectin/anti-CD3 stimulation to activate PBLs from healthy donors, since this method allows efficient proliferation and high-level transgene expression in retrovirally modified T-cells, with less differentiated phenotypes as described previously [20]. Comparative analysis showed that RetroNectin/anti-CD3 treatment mediated *ex vivo* expansion of transduced T-cells to levels comparable to treatment with anti-CD3 and anti-CD28 beads, but was significantly higher than treatment with anti-CD3 alone [20]. Activated PBLs were transduced with SFG-1928z retroviral vectors that encode the 2nd generation of CD19-CAR with the CD28 gene (Fig. 1A), and were selectively propagated on 3T3/CD19 cells. Transduced T-cell numbers increased about 200-fold within two weeks (data not shown). Expression of CD19-CAR$^+$ CD3$^+$ in transduced T-cells was approximately 75%, as assessed by flow cytometry (Fig. 1B). Cellular protein expression of CD19-CAR in transduced T-cells was also confirmed by Western blotting using an anti-CD3ζ antibody (Fig. 1C). We then examined immunophenotypes of CD19-CAR T-cells by flow cytometry. At day 14 of culture, CD19-CAR T-cells predominantly expressed CD8 (75%), compared to the control PBLs without culture (35%) (Fig. S1) as described previously [20]; whereas, anti-CD3 and anti-CD28 beads preferentially induced the CD4$^+$ population (63%), under the same experimental setting (data not shown). While both CD4$^+$ and CD8$^+$ T-cell subsets are targets for CD19-CAR gene transduction, it is not known which subset is suitable for T-cell therapy. Compared to control PBLs without culture, CD19-CAR T-cells cultured with antigen contained primarily central or effector memory subpopulations as exemplified by the co-expression of either CD62L or CCR7 along with CD45RA, or CD27 with CD28 (Fig. S1). Especially noteworthy is the fact that many of the CD19-CAR T-cells were less differentiated (i.e., exhibited a more primitive phenotype), and co-expressed both CD27$^+$ and CD28$^+$, an expression phenotype thought to be suitable for adoptive T-cell transfer [25]. In addition, the lack of CD279 (PD-1) expression (<1%) supports the absence of exhaustion among the CD19-CAR T-cells (data not shown). These results show that large numbers of these cells with high-level transgene expression were generated in our culture conditions.

3.2. CD19-dependent cytokine production and cell lytic activity

We examined the ability of CD19-CAR T-cells to produce cytokines by ELISA and found that they selectively produced IL-2 and IFN-γ in response to CD19$^+$ target cells (Fig. 2A). Cytotoxic assays revealed that they also effectively lysed CD19$^+$ Raji and Daudi cells at increasing effector/target ratios compared to non-transduced T-cells (Fig. 2B). To address the specific killing ability of CD19-CAR T-cells, K562 cells expressing CD19 (K562/CD19) and parental K562 cells (CD19 negative) were used as target cells. As expected, CD19-CAR T-cells lysed CD19$^+$ cells more effectively than CD19$^-$ cells (Fig. S2). Taken together, these results show that expanded CD19-CAR T-cells exhibited CD19-dependent redirected effector functions *in vitro*.

3.3. Accumulation at tumors and anti-tumor activity

To investigate that modified T-cells were able to accumulate at tumor lesions, Rag2$^{-}/\gamma^{-}$ mice with subcutaneous Raji tumors were injected with either CD19-CAR T-cells or non-transduced T-cells. Immunohistochemistry showed that robust accumulation of

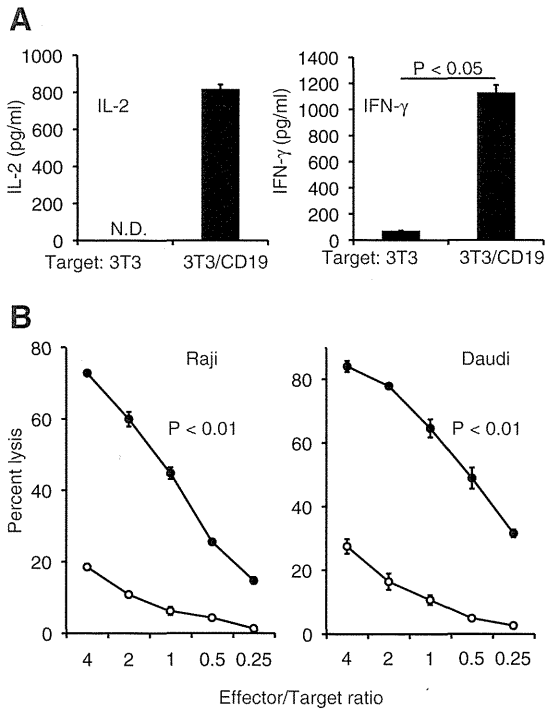

Fig. 2. Antigen-specific cytokine production and cell lytic activity of CD19-CAR T-cells. (A) IL-2 and IFN-γ secretion by CD19-CAR T-cells after co-culture with 3T3/CD19 or the control 3T3 cells ($p < 0.05$). N.D., not detectable. (B) Cell lytic activity of CD19-CAR T-cells (black circles) or the control non-transduced T-cells (white circles) against Raji and Daudi cells in ^{51}Cr release assays. Data show mean ± SD of triplicate wells. CD19-CAR T-cells lysed well compared to non-transduced T-cells at all effector/target ratios ($p < 0.01$).

human CD3$^+$ T-cells occurred at tumor lesions 24 h after administration of CD19-CAR T-cells. A few CD3$^+$ T-cells were detected in control mice (Fig. 3A). Engineered T-cells effectively localized to tumor lesions compared with control T-cells (Fig. 3B). These results are similar to those found for infused T-cells that accumulated at tumors induced by the subcutaneous injection of NALM-6 cells (an ALL cell line) into SCID/beige mice 48 h after T-cell infusion with first generation CD19-CARs [26]. We examined the relationship between accumulation at tumor sites of CD19-CAR T-cells and their anti-tumor effects using a systemic Raji tumor mouse model that we established. When Rag2$^-$/γ^- mice were injected intravenously with Raji/Luc cells, these tumors grew progressively as assessed by bioluminescent imaging. We further confirmed CD19$^+$ tumor infiltration in the spleen, liver and bone marrow by immunohistochemistry (Fig. S3). These infiltrates resembled an aggressive form of human B-cell lymphoma.

For adoptive T-cell therapy, Rag2$^-$/γ^- mice injected intravenously with Raji/Luc cells were subsequently infused with CD19-CAR T-cells. Bioluminescent imaging revealed that the infused cells successfully suppressed Raji tumor progression; whereas, infusion of non-transduced T-cells did not (Fig. 4A), thereby excluding alloreactivity as a mechanism of tumor suppression. Furthermore, mice treated with CD19-CAR T-cells exhibited significantly prolonged survival compared to control cohorts (Fig. 4B). We also examined the ability of infused T-cells to accumulate at tumors in each cohort. Immunohistochemistry revealed more efficient accumulation of human CD3$^+$ T-cells at spleen lesions in mice receiving CD19-CAR T-cells, compared to mice receiving non-transduced T-cells at day 29 (Fig. 4C and D). These results suggest that such cells survive for at least 29 days in tumor bearing-mice, and that the ability of CD19-CAR T-cells to accumulate at tumor lesions is likely associated with the anti-tumor effects observed in human B-cell lymphoma xenograft mouse models.

It is important to note that other parameters, in addition to the accumulation of CD19-CAR T-cells at tumor sites, may also contribute to tumoricidal effects. In CLL patients for example, the localization of CD19-CAR T-cells to tumor lesions was detected by immunohistochemistry up to two months post T-cell infusion, but the accumulation of CAR-modified T-cells at tumor sites was not always consistent with clinical outcomes [7].

In any event, tumor targeting of infused effector T-cells is likely an important prerequisite for CD19-CAR anti-tumor effects. Parameters such as a CAR's structure, scFv antibody region, specific target epitope, and affinity for a given epitope, may be important factors which influence CAR-mediated tumor targeting. In current clinical trials using CD19-CAR T-cells for advanced B-cell malignancies, two types of CD19-CARs expressing either FMC63 or SJ25C1 monoclonal antibody-derived scFvs recognize distinct epitopes with different binding affinities that may play an important role in tumor targeting, anti-tumor effects, and subsequent clinical outcomes [27]. However, there is no direct functional comparison between two CD19-CARs, and critical determinants to select the optimal scFv remain unknown. Recently, Haso et. al. demonstrated that epitope specificity has a major impact on CAR efficacy, since CD22 antigen-specific CARs (CD22-CAR) incorporating an scFv directed to a more membrane proximal epitope, mediated more potent anti-tumor effects in an ALL tumor mouse model than other CD22-CARs of similar affinity, but which targeted distinct epitopes [28]. Thus, the careful selection of a specified CAR antigen epitope is an important consideration towards the improvement of CAR-modified T-cells in eliciting anti-tumor effects. As an alternative approach to efficient tumor targeting of CARs, Craddock et. al. showed that the transfer of CCR2b-chemokine-receptor-expressing CAR-modified T-cells (targeted to GD2 antigen) could enforce preferential migration to tumor lesions, and boost anti-tumor effects in a neuroblastoma mouse model [29]. Therefore, refinement with

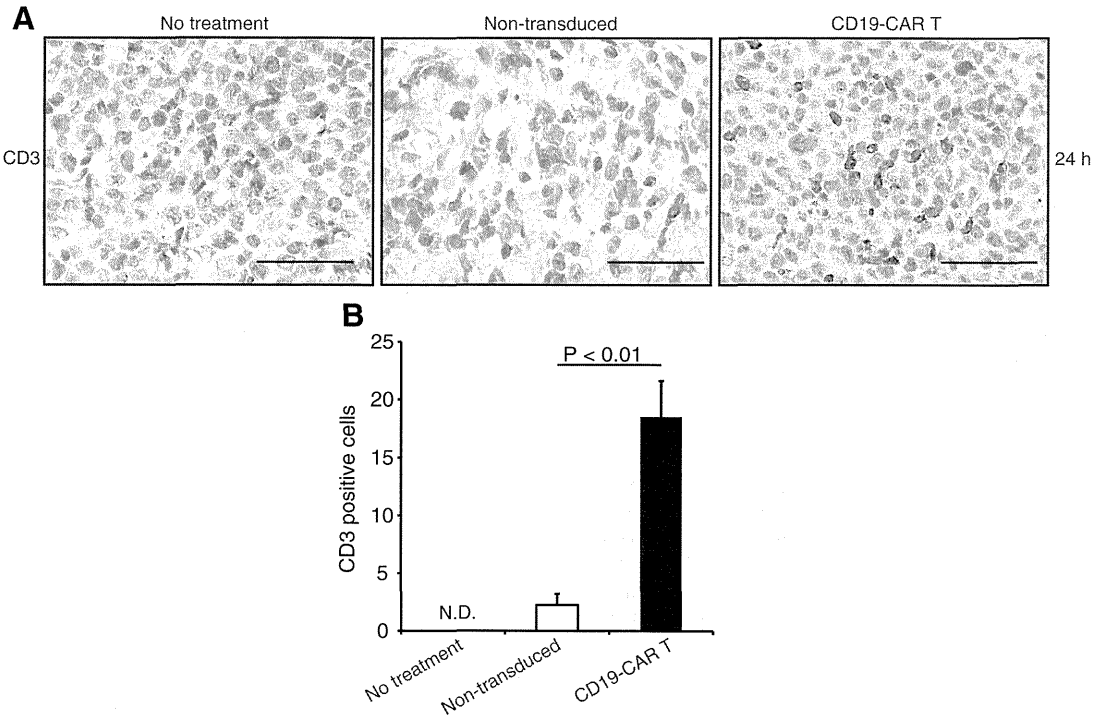

Fig. 3. Accumulation at tumor lesions of CD19-CAR T-cells in subcutaneous xenograft mouse models. (A) Immunohistochemical staining for human CD3 (brown) in subcutaneous Raji tumors from Rag2$^-$/γ^- mice at 24 h after infusion of either CD19-CAR T-cells or the control non-transduced T-cells. Sections from representative mice are shown. (B) CD3$^+$ cell counts in tumor sections from mice receiving CD19-CAR T-cell were higher than those of control sections ($p < 0.01$). Data show mean ± SD of four different fields of view per section. N.D., not detectable. Scale lines, 50 μm. (For interpretation of the references to color in this figure legend, the reader is referred to the web version of this article.)

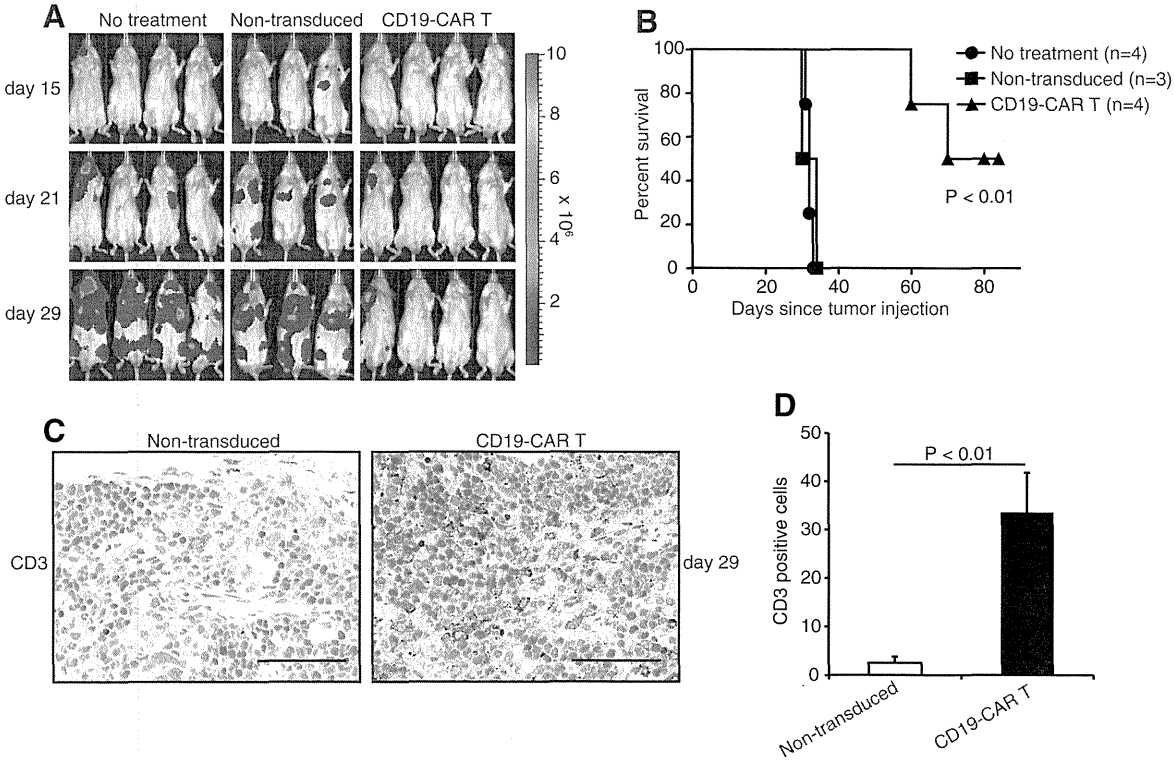

Fig. 4. (A) Bioluminescent imaging of systemic Raji tumor progression in $Rag2^{-}/\gamma^{-}$ mice following T-cell infusion. Mice inoculated intravenously with Raji/Luc cells on day 0, were injected intravenously with either CD19-CAR T-cells or control non-transduced T-cells on day 3. Bioluminescent imaging was performed at days 15, 21 and 29. (B) Enhanced survival of CD19-CAR T-cell-treated mice when compared with the control cohorts ($p < 0.01$). (C) Immunohistochemical staining for human CD3 (brown) in spleen lesions from tumor-bearing mice at day 29 after T-cell administration. (D) $CD3^{+}$ cell counts in tumor sections from mice receiving CD19-CAR T-cell were higher than those of control sections ($p < 0.01$). Data show mean ± SD of four different fields of view per section. Scale lines, 50 μm. (For interpretation of the references to color in this figure legend, the reader is referred to the web version of this article.)

regard to tumor targeting of CAR-modified T-cells may confer enhanced therapeutic potency to CAR-based T-cell therapy.

In conclusion, we have successfully generated large numbers of CD19-CAR T-cells that exhibited antigen-specific cytokine production and cell lytic activity *in vitro*. We also showed that adoptive transfer of these cells strongly suppressed human B-cell lymphoma progression, and this activity correlated with the ability of infused T-cells to accumulate at tumor sites in the xenograft mouse model. These studies expand the repertoire of more potent CD19-CAR-based T-cell therapies for refractory B-cell lymphoma.

Based on our findings here and in other clinical trials [6,7], we will conduct a phase I/II clinical trial, whereby patients with chemorefractory non-Hodgkin B-cell lymphoma will be treated with autologous CD19-CAR T-cells.

Acknowledgments

This work was supported by JSPS KAKENHI Grant Nos. 22700923 to T. Tsukahara; 24390247 to K. Ozawa and Jichi Medical University Young Investigator Award (to T. Tsukahara). This publication was subsidized by JKA through its promotion funds from KEIRIN RACE. We thank Dr. M. Ito (Central Institute for Experimental Animals) for generously providing Balb/c $Rag2^{-/-}\gamma c^{-/-}$ mice. We also thank Gary Baley for critical editing as academic editor.

Appendix A. Supplementary data

Supplementary data associated with this article can be found, in the online version, at http://dx.doi.org/10.1016/j.bbrc.2013.07.030.

References

[1] M.L. Davila, R. Brentjens, X. Wang, I. Riviere, M. Sadelain, How do CARs work?: early insights from recent clinical studies targeting CD19, Oncoimmunology 1 (2012) 1577–1583.
[2] Y.S. Li, R. Wasserman, K. Hayakawa, R.R. Hardy, Identification of the earliest B lineage stage in mouse bone marrow, Immunity 5 (1996) 527–535.
[3] R.J. Brentjens, E. Santos, Y. Nikhamin, R. Yeh, M. Matsushita, K. La Perle, A. Quintas-Cardama, S.M. Larson, M. Sadelain, Genetically targeted T cells eradicate systemic acute lymphoblastic leukemia xenografts, Clin. Cancer Res. 13 (2007) 5426–5435.
[4] C.M. Kowolik, M.S. Topp, S. Gonzalez, T. Pfeiffer, S. Olivares, N. Gonzalez, D.D. Smith, S.J. Forman, M.C. Jensen, L.J. Cooper, CD28 costimulation provided through a CD19-specific chimeric antigen receptor enhances in vivo persistence and antitumor efficacy of adoptively transferred T cells, Cancer Res. 66 (2006) 10995–11004.
[5] M.C. Milone, J.D. Fish, C. Carpenito, R.G. Carroll, G.K. Binder, D. Teachey, M. Samanta, M. Lakhal, B. Gloss, G. Danet-Desnoyers, D. Campana, J.L. Riley, S.A. Grupp, C.H. June, Chimeric receptors containing CD137 signal transduction domains mediate enhanced survival of T cells and increased antileukemic efficacy in vivo, Mol. Ther. 17 (2009) 1453–1464.
[6] R.J. Brentjens, M.L. Davila, I. Riviere, J. Park, X. Wang, L.G. Cowell, S. Bartido, J. Stefanski, C. Taylor, M. Olszewska, O. Borquez-Ojeda, J. Qu, T. Wasielewska, Q. He, Y. Bernal, I.V. Rijo, C. Hedvat, R. Kobos, K. Curran, P. Steinherz, J. Jurcic, T. Rosenblat, P. Maslak, M. Frattini, M. Sadelain, CD19-targeted T cells rapidly induce molecular remissions in adults with chemotherapy-refractory acute lymphoblastic leukemia, Sci. Transl. Med. 5 (2013) 177ra138.
[7] R.J. Brentjens, I. Riviere, J.H. Park, M.L. Davila, X. Wang, J. Stefanski, C. Taylor, R. Yeh, S. Bartido, O. Borquez-Ojeda, M. Olszewska, Y. Bernal, H. Pegram, M. Przybylowski, D. Hollyman, Y. Usachenko, D. Pirraglia, J. Hosey, E. Santos, E. Halton, P. Maslak, D. Scheinberg, J. Jurcic, M. Heaney, G. Heller, M. Frattini, M. Sadelain, Safety and persistence of adoptively transferred autologous CD19-targeted T cells in patients with relapsed or chemotherapy refractory B-cell leukemias, Blood 118 (2011) 4817–4828.
[8] M. Kalos, B.L. Levine, D.L. Porter, S. Katz, S.A. Grupp, A. Bagg, C.H. June, T cells with chimeric antigen receptors have potent antitumor effects and can establish memory in patients with advanced leukemia, Sci. Transl. Med. 3 (2011) 95ra73.
[9] J.N. Kochenderfer, M.E. Dudley, S.A. Feldman, W.H. Wilson, D.E. Spaner, I. Maric, M. Stetler-Stevenson, G.Q. Phan, M.S. Hughes, R.M. Sherry, J.C. Yang, U.S.

Kammula, L. Devillier, R. Carpenter, D.A. Nathan, R.A. Morgan, C. Laurencot, S.A. Rosenberg, B-cell depletion and remissions of malignancy along with cytokine-associated toxicity in a clinical trial of anti-CD19 chimeric-antigen-receptor-transduced T cells, Blood 119 (2012) 2709–2720.
[10] J.N. Kochenderfer, W.H. Wilson, J.E. Janik, M.E. Dudley, M. Stetler-Stevenson, S.A. Feldman, I. Maric, M. Raffeld, D.A. Nathan, B.J. Lanier, R.A. Morgan, S.A. Rosenberg, Eradication of B-lineage cells and regression of lymphoma in a patient treated with autologous T cells genetically engineered to recognize CD19, Blood 116 (2010) 4099–4102.
[11] D.L. Porter, B.L. Levine, M. Kalos, A. Bagg, C.H. June, Chimeric antigen receptor-modified T cells in chronic lymphoid leukemia, N. Engl. J. Med. 365 (2011) 725–733.
[12] B. Savoldo, C.A. Ramos, E. Liu, M.P. Mims, M.J. Keating, G. Carrum, R.T. Kamble, C.M. Bollard, A.P. Gee, Z. Mei, H. Liu, B. Grilley, C.M. Rooney, H.E. Heslop, M.K. Brenner, G. Dotti, CD28 costimulation improves expansion and persistence of chimeric antigen receptor-modified T cells in lymphoma patients, J. Clin. Invest. 121 (2011) 1822–1826.
[13] M.T. Stephan, V. Ponomarev, R.J. Brentjens, A.H. Chang, K.V. Dobrenkov, G. Heller, M. Sadelain, T cell-encoded CD80 and 4-1BBL induce auto- and transcostimulation, resulting in potent tumor rejection, Nat. Med. 13 (2007) 1440–1449.
[14] S. Tammana, X. Huang, M. Wong, M.C. Milone, L. Ma, B.L. Levine, C.H. June, J.E. Wagner, B.R. Blazar, X. Zhou, 4-1BB and CD28 signaling plays a synergistic role in redirecting umbilical cord blood T cells against B-cell malignancies, Hum. Gene Ther. 21 (2010) 75–86.
[15] J. Wang, M. Jensen, Y. Lin, X. Sui, E. Chen, C.G. Lindgren, B. Till, A. Raubitschek, S.J. Forman, X. Qian, S. James, P. Greenberg, S. Riddell, O.W. Press, Optimizing adoptive polyclonal T cell immunotherapy of lymphomas, using a chimeric T cell receptor possessing CD28 and CD137 costimulatory domains, Hum. Gene Ther. 18 (2007) 712–725.
[16] X.S. Zhong, M. Matsushita, J. Plotkin, I. Riviere, M. Sadelain, Chimeric antigen receptors combining 4-1BB and CD28 signaling domains augment PI3kinase/AKT/Bcl-XL activation and CD8+ T cell-mediated tumor eradication, Mol. Ther. 18 (2010) 413–420.
[17] L. Zhen, A.A. King, Y. Xiao, S.J. Chanock, S.H. Orkin, M.C. Dinauer, Gene targeting of X chromosome-linked chronic granulomatous disease locus in a human myeloid leukemia cell line and rescue by expression of recombinant gp91phox, Proc. Natl. Acad. Sci. USA (1993) 9832–9836.
[18] A.D. Miller, J.V. Garcia, N. von Suhr, C.M. Lynch, C. Wilson, M.V. Eiden, Construction and properties of retrovirus packaging cells based on gibbon ape leukemia virus, J. Virol. 65 (1991) 2220–2224.
[19] J.B. Latouche, M. Sadelain, Induction of human cytotoxic T lymphocytes by artificial antigen-presenting cells, Nat. Biotechnol. 18 (2000) 405–409.
[20] S.S. Yu, I. Nukaya, T. Enoki, E. Chatani, A. Kato, Y. Goto, K. Dan, M. Sasaki, K. Tomita, M. Tanabe, H. Chono, J. Mineno, I. Kato, In vivo persistence of genetically modified T cells generated ex vivo using the fibronectin CH296 stimulation method, Cancer Gene Ther. 15 (2008) 508–516.
[21] M. Kannagi, K. Sugamura, H. Sato, K. Okochi, H. Uchino, Y. Hinuma, Establishment of human cytotoxic T cell lines specific for human adult T cell leukemia virus-bearing cells, J. Immunol. 130 (1983) 2942–2946.
[22] K. Ohbo, T. Suda, M. Hashiyama, A. Mantani, M. Ikebe, K. Miyakawa, M. Moriyama, M. Nakamura, M. Katsuki, K. Takahashi, K. Yamamura, K. Sugamura, Modulation of hematopoiesis in mice with a truncated mutant of the interleukin-2 receptor gamma chain, Blood 87 (1996) 956–967.
[23] T. Ohteki, T. Fukao, K. Suzue, C. Maki, M. Ito, M. Nakamura, S. Koyasu, Interleukin 12-dependent interferon gamma production by CD8alpha+ lymphoid dendritic cells, J. Exp. Med. 189 (1999) 1981–1986.
[24] Y. Shinkai, G. Rathbun, K.P. Lam, E.M. Oltz, V. Stewart, M. Mendelsohn, J. Charron, M. Datta, F. Young, A.M. Stall, F.W. Alt, RAG-2-deficient mice lack mature lymphocytes owing to inability to initiate V(D)J rearrangement, Cell 68 (1992) 855–867.
[25] M.E. Dudley, C.A. Gross, M.M. Langhan, M.R. Garcia, R.M. Sherry, J.C. Yang, G.Q. Phan, U.S. Kammula, M.S. Hughes, D.E. Citrin, N.P. Restifo, J.R. Wunderlich, P.A. Prieto, J.J. Hong, R.C. Langan, D.A. Zlott, K.E. Morton, D.E. White, C.M. Laurencot, S.A. Rosenberg, CD8+ enriched "young" tumor infiltrating lymphocytes can mediate regression of metastatic melanoma, Clin. Cancer Res. 16 (2010) 6122–6131.
[26] E.B. Santos, R. Yeh, J. Lee, Y. Nikhamin, B. Punzalan, K. La Perle, S.M. Larson, M. Sadelain, R.J. Brentjens, Sensitive in vivo imaging of T cells using a membrane-bound Gaussia princeps luciferase, Nat. Med. 15 (2009) 338–344.
[27] R.J. Brentjens, K.J. Curran, Novel cellular therapies for leukemia: CAR-modified T cells targeted to the CD19 antigen, Hematol. Am. Soc. Hematol. Educ. Program 2012 (2012) 143–151.
[28] W. Haso, D.W. Lee, N.N. Shah, M. Stetler-Stevenson, C.M. Yuan, I.H. Pastan, D.S. Dimitrov, R.A. Morgan, D.J. FitzGerald, D.M. Barrett, A.S. Wayne, C.L. Mackall, R.J. Orentas, Anti-CD22-chimeric antigen receptors targeting B-cell precursor acute lymphoblastic leukemia, Blood 121 (2013) 1165–1174.
[29] J.A. Craddock, A. Lu, A. Bear, M. Pule, M.K. Brenner, C.M. Rooney, A.E. Foster, Enhanced tumor trafficking of GD2 chimeric antigen receptor T cells by expression of the chemokine receptor CCR2b, J. Immunother. 33 (2010) 780–788.

Cancer Science
The official journal of the Japanese Cancer Association JCA

Suppression of lymph node and lung metastases of endometrial cancer by muscle-mediated expression of soluble vascular endothelial growth factor receptor-3

Kayoko Takahashi,[1,2,4] Hiroaki Mizukami,[1,3] Yasushi Saga,[2] Yuji Takei,[2] Masashi Urabe,[1] Akihiro Kume,[1] Shizuo Machida,[2] Hiroyuki Fujiwara,[2] Mitsuaki Suzuki[2] and Keiya Ozawa[1,3]

[1]Division of Genetics Therapeutics, Center for Molecular Medicine; [2]Department of Obstetrics and Gynecology, Jichi Medical University, Shimotsuke, Japan

(Received February 21, 2013/Revised April 16, 2013/Accepted April 17, 2013/Accepted manuscript online April 24, 2013/Article first published online June 4, 2013)

Lymph node metastasis is the most important prognostic factor of endometrial cancer. However, effective therapy has not been established against lymph node metastasis. In this study, we explored the efficacy of gene therapy targeting lymph node metastasis of endometrial cancer by suppressing the action of vascular endothelial growth factor (VEGF)-C through soluble VEGF receptor-3 (sVEGFR-3) expression. For this purpose, we first conducted a model experiment by introducing sVEGFR-3 cDNA into an endometrial cancer cell line HEC1A and established HEC1A/sVEGFR-3 cell line with high sVEGFR-3 expression. The conditioned medium of HEC1A/sVEGFR-3 cells inhibited lymphatic endothelial cell growth *in vitro*, and sVEGFR-3 expression in HEC1A cells suppressed *in vivo* lymph node and lung metastases without inhibiting the growth of a subcutaneously inoculated tumor. To validate the therapeutic efficacy, adeno-associated virus vectors encoding sVEGFR-3 were injected into the skeletal muscle of mice with lymph node metastasis. Lymph node and lung metastases of HEC1A cells were completely suppressed by the muscle-mediated expression of sVEGFR-3 using adeno-associated virus vectors. These results suggest the possibility of gene therapy against lymph node and lung metastases of endometrial cancer by using muscle-mediated expression of sVEGFR-3. (*Cancer Sci* 2013; 104: 1107–1111)

Endometrial cancer is the most commonly encountered gynecologic malignancy and the fourth most common malignant tumor in the USA.[1] Because this cancer is often detected at an early stage while it is still confined to the uterus, the overall survival rate exceeds 80%.[1] However, the prognosis of advanced endometrial cancer remains poor.[2,3] Although various attempts have been made to treat advanced endometrial cancer, including surgery, radiotherapy and multidrug chemotherapy, satisfactory progress has not been achieved. In fact, overall treatment results in endometrial cancer have not improved over the past 30 years.[1] The most important prognostic factor in endometrial cancer is extrauterine spread, especially lymph node and lung metastases.[4] Therefore, to improve the prognosis of endometrial cancer, it is necessary to develop effective therapy against such advanced conditions.

Factors related to lymphangiogenesis and lymph node metastasis have been clarified recently. Among these factors, vascular endothelial growth factor (VEGF)-C, which is the natural ligand for VEGF receptor-3 (VEGFR-3), is one of the most important. VEGF-C binds to VEGFR-3 and induces its tyrosine autophosphorylation. VEGF-C is specific to the lymphatic vascular system and mediates lymphangiogenesis.[5] In malignant tissues, the tumor cells and stromal cells promote VEGF-C secretion, thereby inducing lymphangiogenesis and lymph node metastasis.[6] The soluble form of VEGFR-3 (sVEGFR-3) is a potent inhibitor of VEGF-C signaling, which inhibits fetal lymphangiogenesis and induces regression of already formed lymphatic vessels.[7] Therefore, lymph node metastasis of a malignant tumor may be controlled by the action of sVEGFR-3.

Recently, we developed a murine model for lymph node metastasis using orthotopic injection of an endometrial cancer cell line.[8] Based on the study, we sought to investigate the efficacy of sVEGFR3 by its constitutive expression. For this purpose, the adeno-associated virus (AAV) vector is appropriate. The AAV is a widely–used vector derived from a nonpathogenic virus, and long-term transgene expression can be obtained following intramuscular injection.[9] We have reported the efficacy of muscle-mediated soluble Flt-1 expression using AAV vectors in both subcutaneous and intraperitoneally disseminated ovarian cancer.[10] In this study, we explored the efficacy of gene therapy against metastases of endometrial cancer by muscle-mediated expression of sVEGFR-3 using AAV vectors.

Materials and Methods

Cells and plasmids. The human endometrial cancer cell line HEC1A[11] was obtained from the Japanese Collection of Research Bioresources, where the cell line is authenticated by the Multiplex-PCR method using short tandem repeats.[12] The HEC1A was cultured in DMEM/F12 (GIBCO, Grand Island, NY, USA) supplemented with 10% inactivated FCS, 100 U/mL of penicillin and 100 μg/mL of streptomycin (GIBCO) at 37°C in a 5% CO_2 atmosphere. Human neonatal dermal lymphatic endothelial cells (LEC) were purchased from Angio-Bio (Del Mar, CA, USA) and maintained in EGM-MV2 BulletKit (Cambrex, East Rutherford, NJ, USA) supplemented with 10% inactivated FCS at 37°C in a 5% CO_2 atmosphere. All cell lines were maintained for less than 3 months after resuscitation. The cDNA of sVEGFR-3 was cloned by PCR using a human lung cDNA library (Stratagene, La Jolla, CA, USA) as a template, with the primers previously described.[7] Cloned sVEGFR-3 cDNA was inserted into the multi-cloning site (MCS) of pSecTagHygroB vector (Stratagene) to generate a VEGFR-3-expression plasmid. A luciferase (LUC)-encoding plasmid was also constructed and used as a control vector.

[3]To whom correspondence should be addressed.
E-mails: miz@jichi.ac.jp; kozawa@jichi.ac.jp
[4]Present address: Department of Obstetrics and Gynecology, International University of Health and Welfare Hospital, Nasushiobara, Japan.

doi: 10.1111/cas.12184

p2ITR-sVEGFR-3 is an sVEGFR-3 expression plasmid prepared by incorporating human sVEGFR-3 cDNA into the EcoRI site of pAAV-MCS (Stratagene).

Development of stably transduced cells. Either an sVEGFR3-expression or a LUC-expression plasmid was introduced into the HEC1A cells using the standard calcium phosphate precipitation method.[13] After transfection, the cells were cultured and selected in the presence of 200 μg/mL of hygromycin B (Invitrogen, Carlsbad, CA, USA). After 4 weeks, the hygromycin B-resistant HEC1A/sVEGFR-3 and HEC1A/LUC cell lines were established and maintained thereafter in the presence of 200 μg/mL of hygromycin B.

Adeno-associated virus vector production. Adeno-associated virus vectors were produced by triple-plasmid transfection to 293 cells (Stratagene) using p2ITR-sVEGFR-3, the helper plasmid for adenovirus genes,[14] and the helper plasmid for AAV1.[15,16] A plasmid encoding human coagulation factor IX (hfIX) gene was used to prepare the control AAV vector.[17] The vector stocks were purified using cesium chloride density-gradient ultracentrifugation, and the titer was determined by dot blot and real-time PCR, as described previously.[18] The primers were designed to amplify the cytomegalovirus promoter sequence, and the forward and reverse primers were 5′-GTA TTT ACG GTA AAC TGC CCA CTT-3′ and 5′-AGT CCC ATA AGG TCA TGT ACT GG-3′, respectively.

Vascular endothelial growth factor-C and soluble vascular endothelial growth factor receptor-3 quantitation. HEC1A, HEC1A/LUC and HEC1A/sVEGFR-3 cells were inoculated in 10-cm dishes and cultured in a 10% FCS-supplemented DMEM/F12 medium. When the cells grew to approximately 80% confluence, the culture supernatant was replaced with serum-free culture medium. After 48 h, the culture supernatant was recovered. The concentration of VEGF-C in the supernatant of HEC1A was determined using a Quantikine Human VEGF-C enzyme-linked immunosorbent assay kit (R&D Systems, Minneapolis, MN, USA). The concentrations of sVEGFR-3 in the supernatant of HEC1A, HEC1A/LUC and HEC1A/sVEGFR3 were determined by DuoSet Human VEGFR-3 (R&D Systems).

Lymphatic endothelial cells proliferation assay. Conditioned media were generated by culturing 1×10^6 HEC1A/LUC cells or HEC1A/sVEGFR-3 cells in 2 mL of serum-free DMEM/F12 for 48 h. LEC (5×10^3/well) were plated in 96-well plates in EGM-MV2 plus 5% FCS containing 50% of either conditioned medium with 100 ng/mL VEGF-C (R&D Systems). LEC proliferation was assessed by a colorimetric assay using Cell Proliferation Kit II (XTT; Boehringer Mannheim Biochemica, Mannheim, Germany) 48 h after plating.

Tumor cell transduction model: subcutaneously inoculated tumor growth. Four to six-week-old female BALB/c nude mice (Japan Clea Laboratories, Tokyo, Japan) were used in the experiment. HEC1A/LUC or HEC1A/sVEGFR-3 cells (5×10^6) were subcutaneously transplanted into the backs of the mice, and tumor sizes were measured once a week using a micrometer caliper. Tumor volume was calculated using the formula: volume = (short diameter)^2 × (long diameter) × 0.5.[19]

Evaluation of metastasis. HEC1A/LUC or HEC1A/sVEGFR-3 cells (5×10^6) were injected into the uterine cavities of pentobarbital sodium-anesthetized, laparotomized mice, as described previously.[8] After 8 weeks, metastatic lesions were thoroughly investigated and counted.

Therapeutic model using adeno-associated virus vector: evaluation of metastasis in orthotopically inoculated model. HEC1A cells (5×10^6) were injected into the uterine cavities of pentobarbital sodium-anesthetized, laparotomized mice, as described previously.[8] At the same time AAV1-hfIX or AAV1-sVEGFR-3 vector (2.5×10^{12} genome copy) was injected into the hindlimb skeletal muscles of the mice. Eight weeks after injection, the metastatic changes were extensively investigated and numbers of enlarged lymph nodes and lung metastases were counted.

Statistical analysis. Intergroup differences were tested for significance using Student's *t*-test. A *P*-value <0.05 was considered significant.

Results

Detection of vascular endothelial growth factor-C and soluble vascular endothelial growth factor receptor-3 in culture supernatants. The concentration of VEGF-C in the culture supernatant of HEC1A cells was 235 ± 12 pg/mL. In the culture supernatant of HEC1A/sVEGFR-3 cells, 45.0 ± 3.2 pg/mL of sVEGFR-3 was detected, but no sVEGFR-3 was detected in the culture supernatant of either HEC1A or HEC1A/LUC cells.

Inhibitory effects of soluble vascular endothelial growth factor receptor-3 on *in vitro* lymphatic endothelial cells growth. The effect of the sVEGFR-3 expression of HEC1A/sVEGFR-3 cells on the action of VEGF-C was estimated using *in vitro* cultures of LEC. The number of LEC in EGM-MV2 culture medium, including 100 ng/mL recombinant VEGF-C plus 50% conditioned medium from HEC1A/sVEGFR-3 cells, was significantly smaller than that in the control (Fig. 1a–c, $P < 0.01$). We concluded that the mitogenic effect of VEGF-C on LEC was abrogated by the presence of sVEGFR-3 in the HEC1A/sVEGFR-3 conditioned medium.

Tumor cell transduction model: subcutaneously inoculated tumor growth. The tumor growth curves of HEC1A/LUC and HEC1A/sVEGFR-3 show no significant differences between the two groups (Fig. 2). This indicates that expression of sVEGFR-3 did not affect the growth of subcutaneously inoculated tumors.

Lymph node metastasis. The effects of sVEGFR-3 gene expression on lymph node metastasis *in vivo* are shown (Fig. 3a–c). The mean number of lymph node metastases 8 weeks after injection was 1.0 ± 0.7 in the control group, but no lymph node metastases were observed in the HEC1A/sVEGFR-3-injected group (Fig. 3c), indicating that sVEGFR-3 inhibited lymph node metastasis of the HEC1A cells.

Lung metastasis. After thorough investigation for metastasis, we noticed lung metastasis in these animals. Therefore, we focused on the number of lung metastases along with the number of lymph node metastases. The effects of sVEGFR-3 gene expression on lung metastasis *in vivo* are summarized in Figure 4. The mean number of lung metastases 8 weeks after injection was 3.8 ± 0.8 in the control group, but no lung metastases were observed in the HEC1A/sVEGFR-3-injected group, indicating that sVEGFR-3 completely inhibited lung metastasis of the HEC1A cells.

Therapeutic model using adeno-associated virus vector. The efficacy of muscle-mediated sVEGFR-3 expression was evaluated in lymph node and lung metastases models using HEC1A cells. As shown in Figure 5, the mean number of lymph node metastases 8 weeks after injection of HEC1A cells was 2.4 ± 0.5 in the control group, while no lymph node metastases were observed in the AAV1-sVEGFR-3-injected group. Moreover, the mean number of lung metastases 8 weeks after injection of HEC1A cells was 5.7 ± 2.1 in the control group, while no lung metastases were observed in the AAV1-sVEGFR-3-injected group (Fig. 6a–c). Thus, we observed a significant therapeutic effect in both lymph node and lung metastases.

Discussion

In this study, we explored the possibility of gene therapy targeted at lymph node and lung metastasis using muscle-mediated expression of sVEGFR-3 as a new treatment modality for advanced endometrial cancer. Our results show that sVEGFR-3 in the conditioned medium of sVEGFR-3-transduced

doi: 10.1111/cas.12184

endometrial cancer cells inhibited LEC growth *in vitro*, and sVEGFR-3 expression in endometrial cancer cells suppressed *in vivo* lymph node and lung metastases, although it did not inhibit the growth of subcutaneously inoculated tumors. In

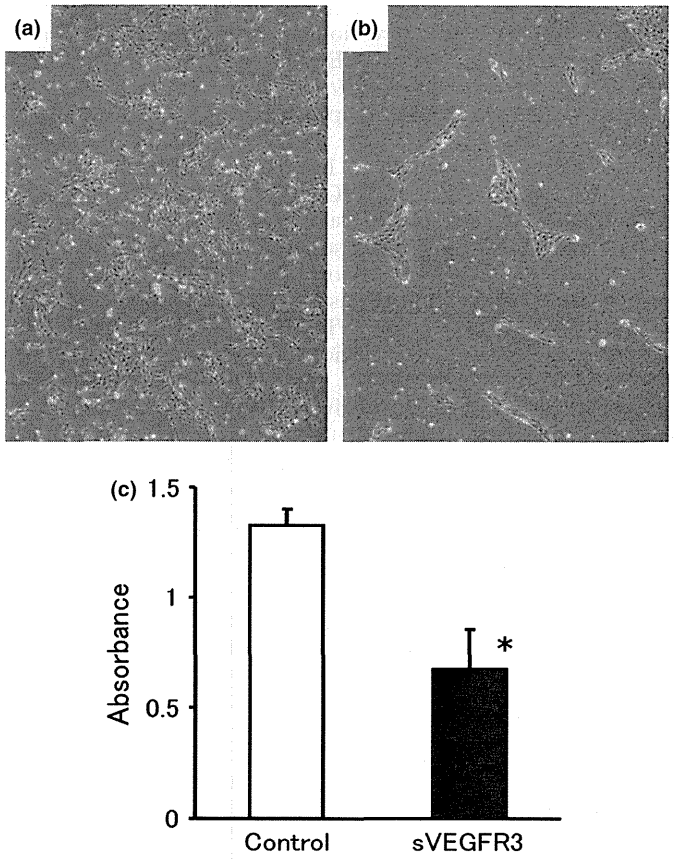

Fig. 1. Suppression of vascular endothelial growth factor (VEGF)-C-driven lymphatic endothelial cell (LEC) proliferation by conditioned medium of soluble vascular endothelial growth factor receptor-3 (sVEGFR-3)-expressing cells. Cells were plated at 5×10^3 cells/well in 96-well plates, and 50% sVEGFR-3-conditioned medium or luciferase-conditioned medium was added with 100 ng/mL recombinant human VEGF-C. The number of LEC with 50% sVEGFR-3-conditioned medium (b) was clearly smaller than that with control (a). The cells were counted by colorimetric assay 48 h after plating. Each bar represents the mean ± SD. (*$P < 0.01$) (c).

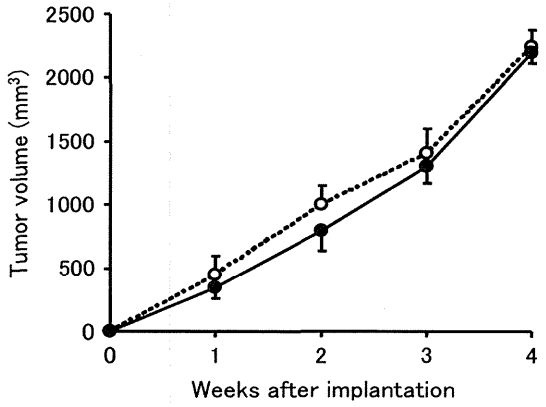

Fig. 2. The tumor growth curves of HEC1A/luciferase and HEC1A /vascular endothelial growth factor receptor-3. Tumor cells were subcutaneously injected into the backs of mice, and the sizes of tumors were measured every week. There were no significant differences between the two groups. Each bar represents the mean ± SD.

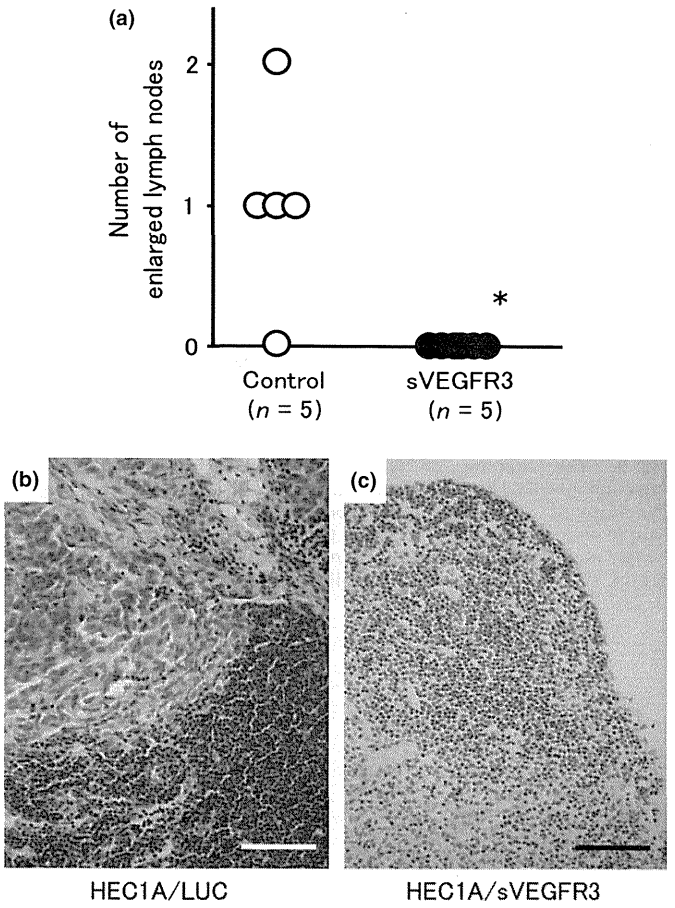

Fig. 3. (a) The number of lymph node metastases 8 weeks after injection of HEC1A/luciferase and HEC1A/vascular endothelial growth factor receptor-3 (sVEGFR-3) cells. Lymph node metastases were observed in the control group (b), while no lymph node metastases were observed in the HEC1A/sVEGFR-3-injected group (c). The mean number of lymph node metastases was 1.0 ± 0.7 in the control group, while no lymph node metastases were observed in the HEC1A/sVEGFR-3-injected group. Bars represent 100 μm.

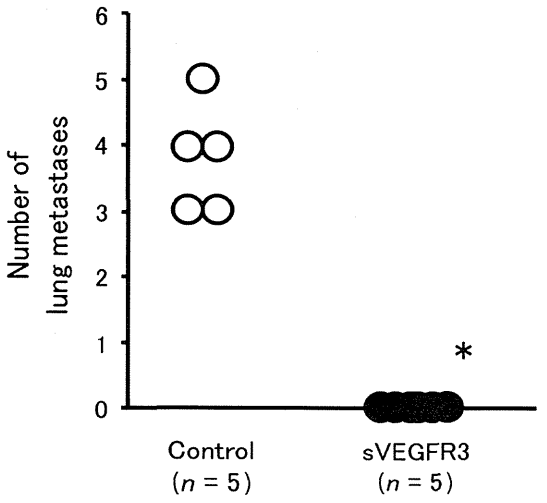

Fig. 4. The number of lung metastases 8 weeks after injection of HEC1A/luciferase and HEC1A/vascular endothelial growth factor receptor-3 (sVEGFR-3) cells. The mean number of lung metastases 8 weeks after injection was 3.8 ± 0.8 in the control group, while no lung metastases were observed in the HEC1A/sVEGFR-3-injected group.

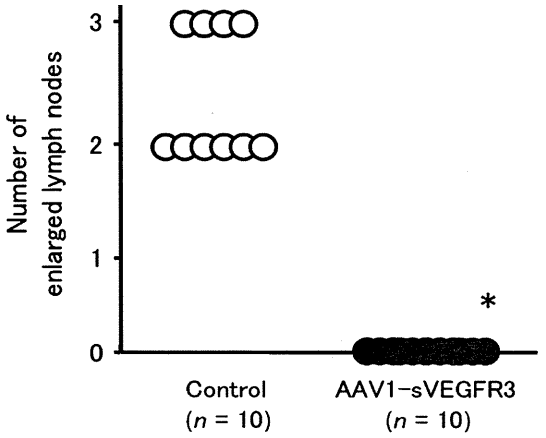

Fig. 5. The number of lymph node metastases 8 weeks after injection of HEC1A cells in the mice that had received intramuscular injections of AAV1-sVEGFR-3 or control vector. The mean number of lymph node metastases was 2.4 ± 0.5 in the control group, while no lymph node metastases were observed in the AAV1-sVEGFR-3-injected group. sVEGFR-3, vascular endothelial growth factor receptor-3.

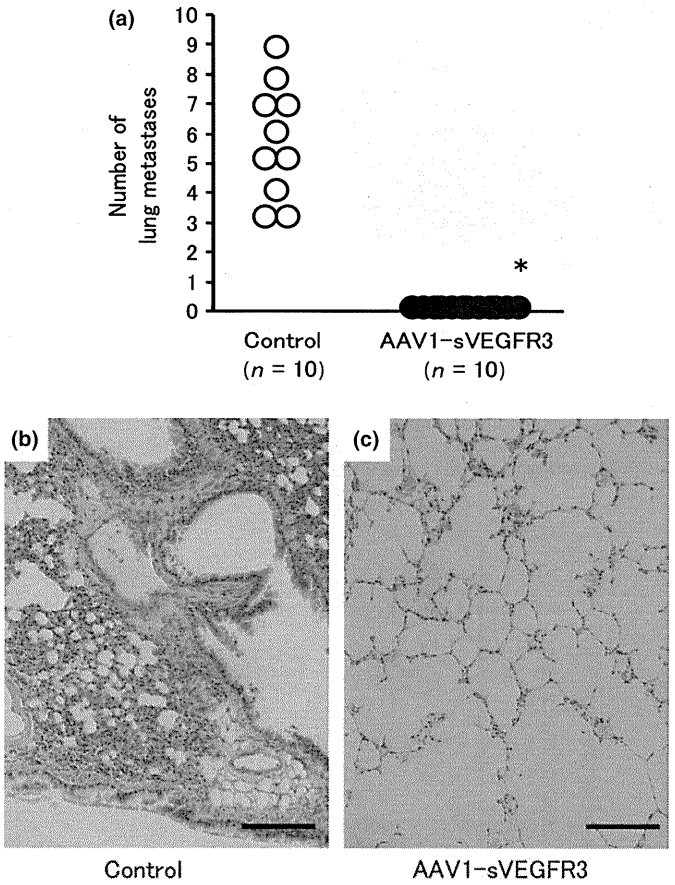

Fig. 6. Lung metastases 8 weeks after injection of HEC1A cells in the mice that had received intramuscular injections of AAV1-sVEGFR-3 or control vector. The mean number of lung metastases was 5.7 ± 2.1 in the control group, while no lung metastases were observed in the AAV1-sVEGFR-3-injected group (a). Lung metastases were observed in the control group (b), while no lung metastases were observed in the AAV1-sVEGFR-3-injected group (c). Bars represent 100 μm. sVEGFR-3, vascular endothelial growth factor receptor-3.

addition, lymph node and lung metastases of endometrial cancer cells were suppressed by muscle-mediated expression of sVEGFR-3 using AAV vectors.

Lymph node metastasis is the most important prognostic factor in endometrial cancer.[3,20] In this study, we tested the efficacy of a gene therapy strategy using sVEGFR-3 to suppress lymph node metastasis through VEGF-C inhibition. We first introduced sVEGFR-3 cDNA into an endometrial cancer cell line HEC1A and established a cell line (HEC1A/sVEGFR-3) with high expression of sVEGFR-3 to investigate its function. The growth of HEC1A/sVEGFR-3 did not show any difference in either *in vitro* cell proliferation (data not shown) or *in vivo* tumor expansion (Fig. 2), showing that overexpression of sVEGFR-3 did not influence the spread of endometrial cancer *per se*. In contrast, in the lymph node metastasis model using HEC1A/sVEGFR-3, lymph node metastasis was completely suppressed. Moreover, in this model, lung metastasis was also completely eliminated. Thus, we demonstrated that expression of sVEGFR-3 could control lymph node and lung metastases of endometrial cancer. Because the expression of sVEGFR-3 did not influence the growth of HEC1A cells, its action was confined to the suppression of lymph node metastasis. The VEGF-C in culture supernatant is thought to be derived from HEC1A cells, and accumulated during cell culture. In fact, we demonstrated various but similar concentrations of VEGF-C in tumor cell culture supernatant.[8] In contrast, soluble VEGFR3 was demonstrated specifically to the cells transduced by sVEGFR3 gene, as shown in the Results section.

Based on these findings, we aimed to establish a gene therapy using sVEGFR-3. For this purpose, we compared the utility of candidate vectors to attain this goal. Non-viral vectors are easier to prepare, and may be safer, but the efficacy is much weaker than viral vectors. Successful *in vivo* delivery has been limited.[21]. As for the viral vectors, many successful outcomes in clinical trials have been reported.[22] For the current study, we chose an AAV1-based vector, as it appears to be the most efficient in muscle transduction.[9,15,23] The result was that both lymph node and lung metastases of endometrial cancer cells were completely suppressed by muscle-mediated expression of sVEGFR-3. These results suggest the possibility of gene therapy targeting lymph node and lung metastases of endometrial cancer by muscle-mediated expression of sVEGFR-3. In the case of AAV vectors, a couple of weeks may be necessary for maximal transgene expression.[22,24–26] Nonetheless, as sufficient levels of expression can last over the observation period of 8 weeks, a significant outcome was obtained even when the vector was administered simultaneously to the tumor inoculation. In this study, we selected muscle tissue for gene expression. For the clinical translation, other tissues may be more appropriate: for example, liver can be efficiently targeted by AAV8 vector[26] and adipose tissue can be targeted by AAV1 vectors.[24]

This study aimed to suppress actions of VEGF-C through the expression of a soluble form of its receptor, sVEGFR3. Therefore, lymph node metastasis was suppressed as a result of lymphangiogenesis inhibition. However, because this treatment did not suppress primary tumor growth, it may be necessary to combine it with other treatment modalities such as surgery and chemotherapy in clinical practice. One recent study utilized chemotherapeutic reagents in addition to gene therapy using soluble VEGF receptors for prolonged survival in mice.[27]

Recently, we developed a lymph node metastasis model using orthotopic injection of endometrial cancer.[8] In that report, only lymph node metastasis was noted. During the current series of experiments, metastatic foci of the lungs could barely be recognized from the surface, and we noticed lung metastasis after extensive microscopic examination. Therefore, the number of metastasis was counted based on the microscopic examination of the tissue sections. As for lung

doi: 10.1111/cas.12184

metastasis, both lymphatic and hematogenous routes are known. It is not easy to determine the route of metastasis solely by histopathological examination. Nonetheless, we assume that in human endometrial cancer, the main route of lung metastasis is lymphatic as lymph node metastasis is detected in more than half of the patients with lung metastasis.[28] Also, in the present study, lung metastasis of endometrial cancer was completely suppressed as a result of controlling lymph node metastasis with sVEGFR-3.

In this study, we demonstrated the efficacy of sVEGFR-3 at one vector dose. As both lymph node and lung metastasis were completely eliminated, there is a possibility that the therapeutic efficacy can be demonstrated at lower vector doses. In addition, in our observation, no side effects were noted in the mice, including in behavior, body weight and muscle tissue. However, for application to human therapy, these points need to be clarified in more detail.

Few studies concerning molecular-targeted therapy or gene therapy for endometrial cancer have been reported. Gene therapy against lymph node and lung metastases, which we propose here, could be beneficial for patients with advanced endometrial cancer. New therapeutic modalities, including this one, are expected to result in improved outcomes for endometrial cancer.

Acknowledgments

This study was supported by Grants-in-Aid for Scientific Research (17016067 and 21591248) and the Support Program for Strategic Research Infrastructure from the Japanese Ministry of Education, Culture, Sports, Science and Technology and the Ministry of Health, Labor and Welfare, Japan.

Disclosure Statement

The authors have no conflict of interest.

References

1 Siegel R, Ward E, Brawley O, Jemal A. Cancer statistics, 2011: the impact of eliminating socioeconomic and racial disparities on premature cancer deaths. *CA Cancer J Clin* 2011; **61**: 212–36.
2 Amant F, Moerman P, Neven P, Timmerman D, Van Limbergen E, Vergote I. Endometrial cancer. *Lancet* 2005; **366**: 491–505.
3 Wolfson AH, Sightler SE, Markoe AM *et al.* The prognostic significance of surgical staging for carcinoma of the endometrium. *Gynecol Oncol* 1992; **45**: 142–6.
4 Lurain J. Uterine cancer. In: Berec J, ed. *Novak's Gynecology*, 12th edn. Baltimore: Williams & Wilkins, 1996; 1057–77.
5 Makinen T, Veikkola T, Mustjoki S *et al.* Isolated lymphatic endothelial cells transduce growth, survival and migratory signals via the VEGF-C/D receptor VEGFR-3. *EMBO J* 2001; **20**: 4762–73.
6 Skobe M, Hawighorst T, Jackson DG *et al.* Induction of tumor lymphangiogenesis by VEGF-C promotes breast cancer metastasis. *Nat Med* 2001; **7**: 192–8.
7 Makinen T, Jussila L, Veikkola T *et al.* Inhibition of lymphangiogenesis with resulting lymphedema in transgenic mice expressing soluble VEGF receptor-3. *Nat Med* 2001; **7**: 199–205.
8 Takahashi K, Saga Y, Mizukami H *et al.* Development of a mouse model for lymph node metastasis with endometrial cancer. *Cancer Sci* 2011; **102**: 2272–7.
9 Mueller C, Flotte TR. Clinical gene therapy using recombinant adeno-associated virus vectors. *Gene Ther* 2008; **15**: 858–63.
10 Takei Y, Mizukami H, Saga Y *et al.* Suppression of ovarian cancer by muscle-mediated expression of soluble VEGFR-1/Flt-1 using adeno-associated virus serotype 1-derived vector. *Int J Cancer* 2007; **120**: 278–84.
11 Kuramoto H, Tamura S, Notake Y. Establishment of a cell line of human endometrial adenocarcinoma in vitro. *Am J Obstet Gynecol* 1972; **114**: 1012–9.
12 Tanabe H, Takada Y, Minegishi D, Kurematsu M, Masui T, Mizusawa H. Cell line individualization by STR multiplex system in the cell bank found cross contamination between ECV304 and EJ-1/T24. *Tiss Cult Res Commun* 1999; **18**: 329–38.
13 Takei Y, Saga Y, Mizukami H *et al.* Overexpression of PTEN in ovarian cancer cells suppresses i.p. dissemination and extends survival in mice. *Mol Cancer Ther* 2008; **7**: 704–11.
14 Matsushita T, Elliger S, Elliger C *et al.* Adeno-associated virus vectors can be efficiently produced without helper virus. *Gene Ther* 1998; **5**: 938–45.
15 Mochizuki S, Mizukami H, Kume A *et al.* Adeno-associated virus (AAV) vector-mediated liver- and muscle-directed transgene expression using various kinds of promoters and serotypes. *Gene Ther Mol Biol* 2004; **8**: 9–18.
16 Xiao W, Chirmule N, Berta SC, McCullough B, Gao G, Wilson JM. Gene therapy vectors based on adeno-associated virus type 1. *J Virol* 1999; **73**: 3994–4003.
17 Ogura T, Mizukami H, Mimuro J *et al.* Utility of intraperitoneal administration as a route of AAV serotype 5 vector-mediated neonatal gene transfer. *J Gene Med* 2006; **8**: 990–7.
18 Ishiwata A, Mimuro J, Mizukami H *et al.* Liver-restricted expression of the canine factor VIII gene facilitates prevention of inhibitor formation in factor VIII-deficient mice. *J Gene Med* 2009; **11**: 1020–9.
19 Kung AL, Wang S, Klco JM, Kaelin WG, Livingston DM. Suppression of tumor growth through disruption of hypoxia-inducible transcription. *Nat Med* 2000; **6**: 1335–40.
20 Lurain JR, Rice BL, Rademaker AW, Poggensee LE, Schink JC, Miller DS. Prognostic factors associated with recurrence in clinical stage I adenocarcinoma of the endometrium. *Obstet Gynecol* 1991; **78**: 63–9.
21 Zhang Y, Satterlee A, Huang L. In vivo gene delivery by nonviral vectors: overcoming hurdles? *Mol Ther* 2012; **20**: 1298–304.
22 Giacca M, Zacchigna S. Virus-mediated gene delivery for human gene therapy. *J Control Release* 2012; **161**: 377–88.
23 Chao H, Liu Y, Rabinowitz J, Li C, Samulski RJ, Walsh CE. Several log increase in therapeutic transgene delivery by distinct adeno-associated viral serotype vectors. *Mol Ther* 2000; **2**: 619–23.
24 Mizukami H, Mimuro J, Ogura T *et al.* Adipose tissue as a novel target for in vivo gene transfer by adeno-associated viral vectors. *Hum Gene Ther* 2006; **17**: 921–8.
25 Flotte TR, Trapnell BC, Humphries M *et al.* Phase 2 clinical trial of a recombinant adeno-associated viral vector expressing alpha1-antitrypsin: interim results. *Hum Gene Ther* 2011; **22**: 1239–47.
26 Nathwani AC, Tuddenham EG, Rangarajan S *et al.* Adenovirus-associated virus vector-mediated gene transfer in hemophilia B. *N Engl J Med* 2011; **365**: 2357–65.
27 Sopo M, Anttila M, Sallinen H *et al.* Antiangiogenic gene therapy with soluble VEGF-receptors -1, -2 and -3 together with paclitaxel prolongs survival of mice with human ovarian carcinoma. *Int J Cancer* 2012; **131**: 2394–401.
28 Otsuka I, Ono I, Akamatsu H, Sunamori M, Aso T. Pulmonary metastasis from endometrial carcinoma. *Int J Gynecol Cancer* 2002; **12**: 208–13.